



HAL
open science

History of the clay-rich unit at Mawrth Vallis, Mars: High-resolution mapping of a candidate landing site

D. Loizeau, N. Mangold, F. Poulet, J. -P. Bibring, J. L. Bishop, J. Michalski,
Cathy Quantin

► To cite this version:

D. Loizeau, N. Mangold, F. Poulet, J. -P. Bibring, J. L. Bishop, et al.. History of the clay-rich unit at Mawrth Vallis, Mars: High-resolution mapping of a candidate landing site. *Journal of Geophysical Research. Planets*, 2015, 120 (11), pp.1820-1846. 10.1002/2015JE004894 . hal-02341064

HAL Id: hal-02341064

<https://univ-lyon1.hal.science/hal-02341064>

Submitted on 1 Jan 2022

HAL is a multi-disciplinary open access archive for the deposit and dissemination of scientific research documents, whether they are published or not. The documents may come from teaching and research institutions in France or abroad, or from public or private research centers.

L'archive ouverte pluridisciplinaire **HAL**, est destinée au dépôt et à la diffusion de documents scientifiques de niveau recherche, publiés ou non, émanant des établissements d'enseignement et de recherche français ou étrangers, des laboratoires publics ou privés.

Copyright

RESEARCH ARTICLE

10.1002/2015JE004894

Key Points:

- High-resolution data enable high-precision geological mapping at Mawrth Vallis
- Mapping shows the variety of depositional and alteration environments
- Highlights the interest of Mawrth Vallis as a future landing site

Correspondence to:

D. Loizeau,
icdamien@gmail.com

Citation:

Loizeau, D., N. Mangold, F. Poulet, J.-P. Bibring, J. L. Bishop, J. Michalski, and C. Quantin (2015), History of the clay-rich unit at Mawrth Vallis, Mars: High-resolution mapping of a candidate landing site, *J. Geophys. Res. Planets*, *120*, 1820–1846, doi:10.1002/2015JE004894.

Received 21 JUL 2015

Accepted 15 OCT 2015

Accepted article online 20 OCT 2015

Published online 21 NOV 2015

History of the clay-rich unit at Mawrth Vallis, Mars: High-resolution mapping of a candidate landing site

D. Loizeau¹, N. Mangold², F. Poulet³, J.-P. Bibring³, J. L. Bishop⁴, J. Michalski⁵, and C. Quantin¹

¹LGLTPE, Université de Lyon, Villeurbanne, France, ²LPNG/CNRS, Nantes, France, ³IAS, Paris XI-Paris Sud, Orsay, Orsay, France, ⁴SETI, Mountain View, California, USA, ⁵PSI, NHM, London, UK

Abstract The Mawrth Vallis region is covered by some of the largest phyllosilicate-rich outcrops on Mars, making it a unique window into the past history of Mars in terms of water alteration, potential habitability, and the search for past life. A landing ellipse had been proposed for the Curiosity rover. This area has been extensively observed by the High Resolution Imaging Science Experiment and the Compact Reconnaissance Imaging Spectrometer for Mars, offering the possibility to produce geologic, structural, and topographic maps at very high resolution. These observations provide an unprecedented detailed context of the rocks at Mawrth Vallis, in terms of deposition, alteration, erosion, and mechanical constraints. Our analyses demonstrate the presence of a variety of alteration environments on the surface and readily accessible to a rover, the presence of flowing water at the surface postdating the formation of the clay-rich units, and evidence for probable circulation of fluids in the rocks at different depths. These rocks undergo continuous erosion, creating fresh outcrops where potential biomarkers may have been preserved. The diversity of aqueous environments over geological time coupled to excellent preservation properties make the area a very strong candidate for future robotic investigation on Mars, like the NASA Mars 2020 mission.

1. Introduction

The Mawrth Vallis region lies at the western limit of Arabia Terra, at the border of Chryse Planitia. This is one of the lowest parts of the Martian highlands, lying between -1500 m and -4000 m in elevation. These plateaus are highly cratered and eroded by the Mawrth Vallis outflow channel. This region was previously mapped as Early and Middle Noachian highland units [Tanaka *et al.*, 2014].

The area (Figure 1) contains some of the largest outcrops of phyllosilicate-rich rocks on Mars [Poulet *et al.*, 2005; Loizeau *et al.*, 2007]. The plateaus of this region include numerous exposures of thick (>150 m), finely layered (layer thickness <10 m), light-toned clay-rich units [Loizeau *et al.*, 2007; Michalski and Noe Dobrea, 2007], formed during the Noachian, >3.7 Ga ago [Loizeau *et al.*, 2012], corresponding to the Phyllosian era as proposed by Bibring *et al.* [2006]. The main clay-rich outcrops cover a region as large as 400 km \times 500 km, spanning elevations from -1500 m to -3500 m, while clay-rich outcrops are also found on the floor of Oyama crater, near the middle of Figure 1, around -3900 m in elevation [Loizeau *et al.*, 2007]. Smaller clay-rich outcrops are also found in a larger region around Mawrth Vallis (~ 1000 km \times 1000 km) [Noe Dobrea *et al.*, 2010]. Fe smectites, Al smectites, and micas [Poulet *et al.*, 2005; Loizeau *et al.*, 2007; Poulet *et al.*, 2014], kaolinite, hydrated silica [Bishop *et al.*, 2008; McKeown *et al.*, 2009; Poulet *et al.*, 2014], and sulfates [Farrand *et al.*, 2009; Wray *et al.*, 2010; Farrand *et al.*, 2014] have been detected within this layered unit through analyses of OMEGA (the Observatoire pour la Minéralogie, l'Eau, les Glaces et l'Activité on board Mars Express [Bibring *et al.*, 2004]) and CRISM (the Compact Reconnaissance Imaging Spectrometer for Mars on board Mars Reconnaissance Orbiter, MRO [Murchie *et al.*, 2007]) spectral imagery. Most of the outcrops show a constant compositional stratigraphy with the Al clay minerals/hydrated silica on top of the Fe clay minerals, the clay-sequence being covered by an anhydrous dark cap unit [Wray *et al.*, 2008; Bishop *et al.*, 2008; Loizeau *et al.*, 2010]. Sulfates are observed in the region, near Mawrth Vallis' mouth, as possible evaporites of jarosite in local lows [Farrand *et al.*, 2009; Michalski *et al.*, 2013] and as scattered outcrops of another Fe sulfate (spectrally similar to copiapite). Sulfates were also identified in deeper layers on the floor of Mawrth Vallis (possible bassanite) [Wray *et al.*, 2010].

Age estimation based on crater counting from Loizeau *et al.* [2012] dates deposition and alteration of the layered unit to the Early to Late Noachian. Part of the clay unit has been eroded away during the Late

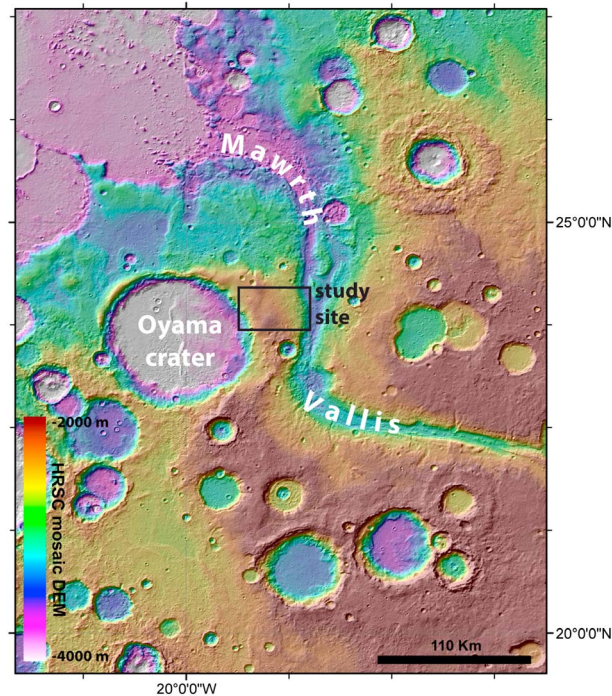


Figure 1. Mawrth Vallis is an outflow valley in the western Arabia Terra, as seen on this HRSC stereo colored shaded relief. Large clay-rich outcrops are detected on the plateaus around the valley and in some craters like Oyama crater [e.g., Loizeau *et al.*, 2007]. The white box shows the location of the study site in the following maps, it had been proposed as a landing site for the NASA Mars Science Laboratory mission. North is up in all figures.

Noachian (~3.8 Ga ago) through fluvial activity and the outflow of Mawrth Vallis. Eroded clays have been redeposited in some places, like on the floor of Oyama crater. The Al clays/hydrated silica at the top of the section were formed after the formation of Mawrth Vallis. This was followed by the dark cap on top of the clay unit, and the infilling of Chryse Planitia during the Early Hesperian, ~3.7 to ~3.6 Ga ago. These ages are given by the chronology model from Hartmann and Neukum [2001].

Hypotheses of deposition propose the accumulation of layers of sediments (aeolian or fluvial deposits in a paleobasin or at the margin of the highlands) or of airfall deposits (dust or volcanoclastic deposits).

Proposed scenarios of alteration for the transition from Fe clays to the Al clays/hydrated silica involve a change in water chemistry, a change in material being altered, a thick alteration profile where the upper clays were leached at a higher degree than the clays below [e.g., Bishop *et al.*, 2013], or an alteration in an ice-dust mixture through briny solutions [Michalski *et al.*, 2013]. The presence of similar clay sequences with Al clays over Fe/Mg clays in various regions of the planet strengthens

the idea of a global weathering episode during a wetter period in the Noachian [Carter *et al.*, 2015]. Sulfates occurring stratigraphically above clays [Farrand *et al.*, 2009] could be relics of a global environmental shift between clay-forming and sulfate-forming epochs [Bibring *et al.*, 2006].

A large fraction of clay minerals in the composition of the layered unit has been inferred from OMEGA's near-infrared (IR) spectral imagery data sets: an unmixing modeling technique estimates clay mineral abundances as high as 50% for many outcrops, the highest abundances identified on Mars so far from orbit [Poulet *et al.*, 2008; Poulet *et al.*, 2014], providing an intriguing and unique window into the hydrogeologic history of early Mars.

Because clay minerals are in many ways favorable to the organization and preservation of organic matter, these deposits have a high preservation potential for biosignatures [Bishop *et al.*, 2013], making Mawrth Vallis an important target for missions seeking to investigate past habitable environments and searching for biomarkers. It was among the four final candidate landing sites for the 2011 Mars Science Laboratory (MSL) mission [Michalski *et al.*, 2010; Golombek *et al.*, 2012] and is a reference landing site for the Mars Sample Return mission [MSR End-to-End International Science Analysis Group, 2011]. In this respect, the proposed landing ellipse has been studied in depth, with complete coverage with high-resolution data sets being acquired, in particular with the HiRISE camera (High Resolution Imaging System on board MRO [McEwen *et al.*, 2007]) and the CRISM imaging spectrometer. A mosaic of CRISM-targeted observations shows large surfaces of Al clays and Fe clays [Bishop *et al.*, 2013]. This data set enables an unprecedented high-precision geologic study from orbit.

A mission based on a similar rover and landing system is planned by NASA for a launch in 2020. It should have prime objectives related to astrobiology and past habitability, looking for a landing site that could have preserved potential biosignatures, and provide well-documented samples for future return to Earth [Mustard *et al.*, 2013]. It is already established that the Mawrth Vallis site represents a habitable region that would be a viable candidate for any future mission tasked with investigating astrobiology [e.g., Bishop *et al.*, 2013].

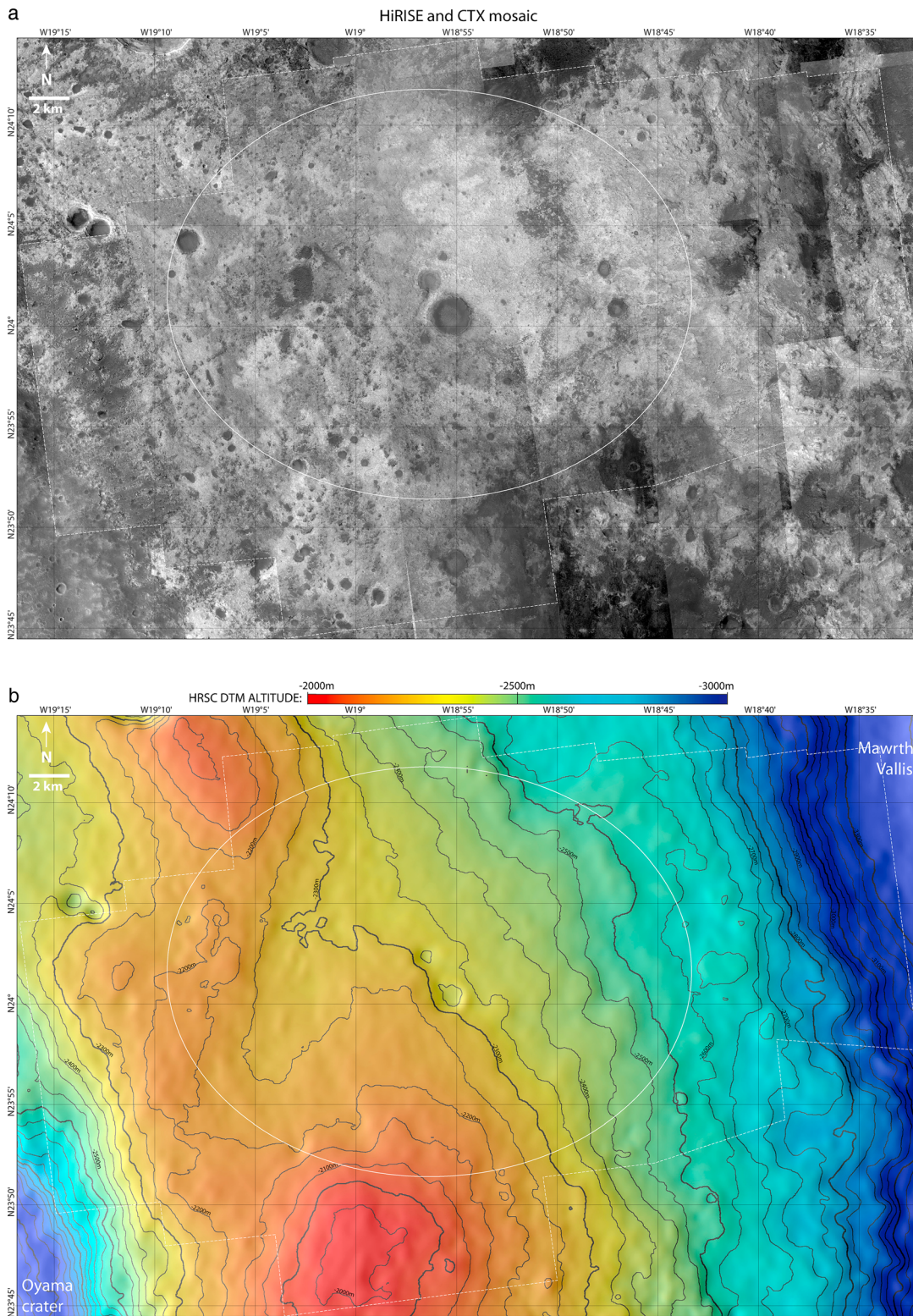


Figure 2. (a) HiRISE mosaic superimposed on CTX images of the study site. The 25 km × 20 km landing ellipse that had been proposed for MSL is represented as a white ellipse. The boundary of the maps of Figures 3 and 4 is also shown with a dashed white line. (b) HRSC DTM in color of the study site with height levels every 50 m and shaded relief. The Mawrth Vallis to the east and the Oyama crater wall to the west are clearly visible in blue. A 250 m high hill is also present to the south of the site. The 25 km × 20 km landing ellipse that had been proposed for MSL is represented as a white ellipse. The boundary of the maps of Figures 3 and 4 is also shown with a dashed white line. (c) CRISM FRT mosaic over CTX modified from *Bishop et al.* [2013]. The Fe/Mg smectite unit appears in orange/red, the ferrous boundary region in green/yellow and the upper Al-/Si-rich unit in blue. (d) HRSC RGB (composed with the red, green, and blue channels, the IR channel was not used) mosaic of the study site.

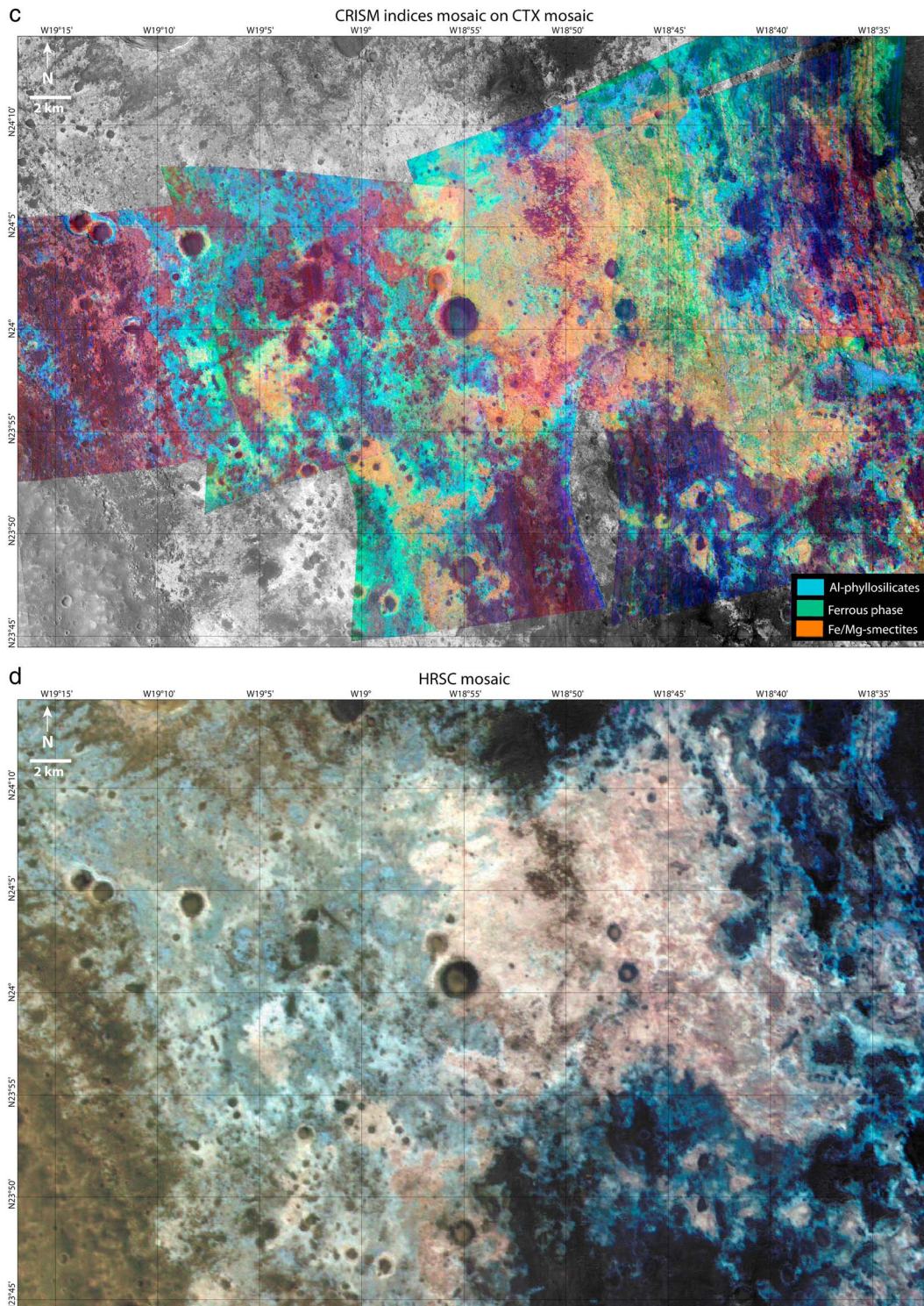


Figure 2. (continued)

The particular area studied here encompasses the MSL candidate landing site ellipse, which was specifically targeted on a large surface of some of the flattest clay-rich rocks of the Mawrth Vallis region. This site exhibits strong spectral signatures of clays and contains one of the “cleanest” areas of clay-rich rocks of the region, with the smallest amount of dust and capping unit.

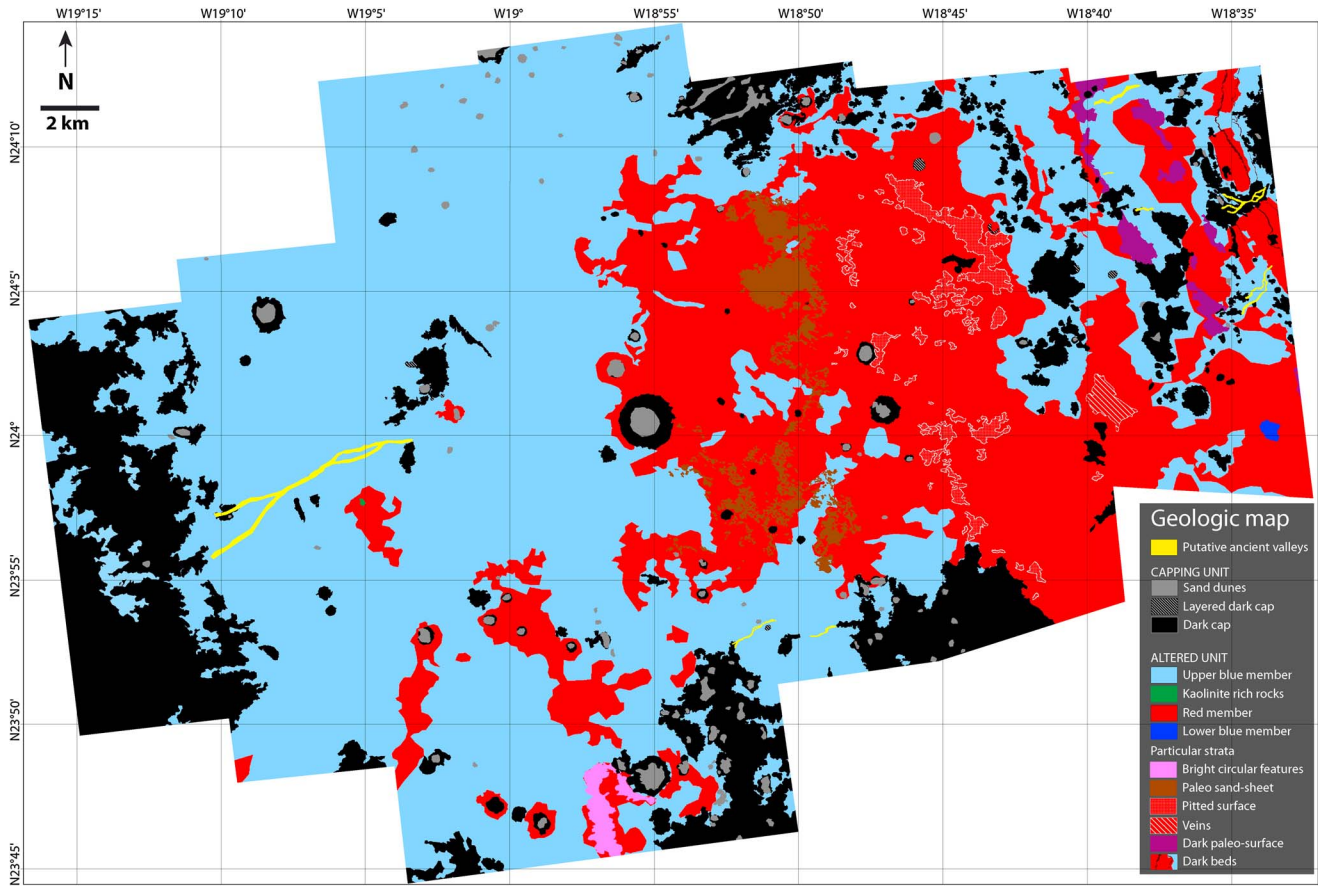


Figure 3. Geologic map of the study site. The map displays the capping unit and the altered unit and their submembers, as well as putative ancient valleys.

In the context of future in situ exploration, our objective is to bring the most advanced knowledge of the candidate landing ellipse (25 × 20 km) using the highest-resolution remote-sensing data obtained to date. Further, this provides a fine understanding of the geology of the site that could be completed by future in situ rover exploration in support of potential samples to be returned to Earth.

To understand the geology of the proposed landing site for MSL, we investigated the surface of the MSL landing ellipse and close surroundings using the mosaics from CTX (Context Camera on board MRO [Malin et al., 2007]), HiRISE, and CRISM. A geologic map and a structural map have been drawn based on the available images at the highest possible resolution. These maps are fundamental for a synthetic view of the geology of the study site, both to get a better knowledge of its geologic history and to prepare for possible future in situ science. What is the detailed stratigraphy of the site, and what does it tell us of the dynamic of deposition there? What are the episodes of alteration that occurred at the site, and did it happen mainly at the surface or in the subsurface? What does the erosion tell us of the water activity at the site too? Did the presence of the large Oyama crater have an influence on the clay units? What is the diversity of past environments that is present? Where is the highest concentration and preservation potential for biosignatures? We present maps and details about the different mapped units and features and discuss the possible formation scenarios based on these high-resolution observations.

2. Data Sets and Mapping Method

2.1. Data Sets

We mosaicked and superimposed available HiRISE images on CTX images (Figure 2a). CTX offers a full coverage of the region of Mawrth Vallis at around 6 m/pixel, while a dense coverage with HiRISE provides almost a full coverage of the study area at a resolution better than 30 cm/pixel. HiRISE also offers partial color coverage. The landing ellipse that had been proposed for the MSL mission is also indicated.

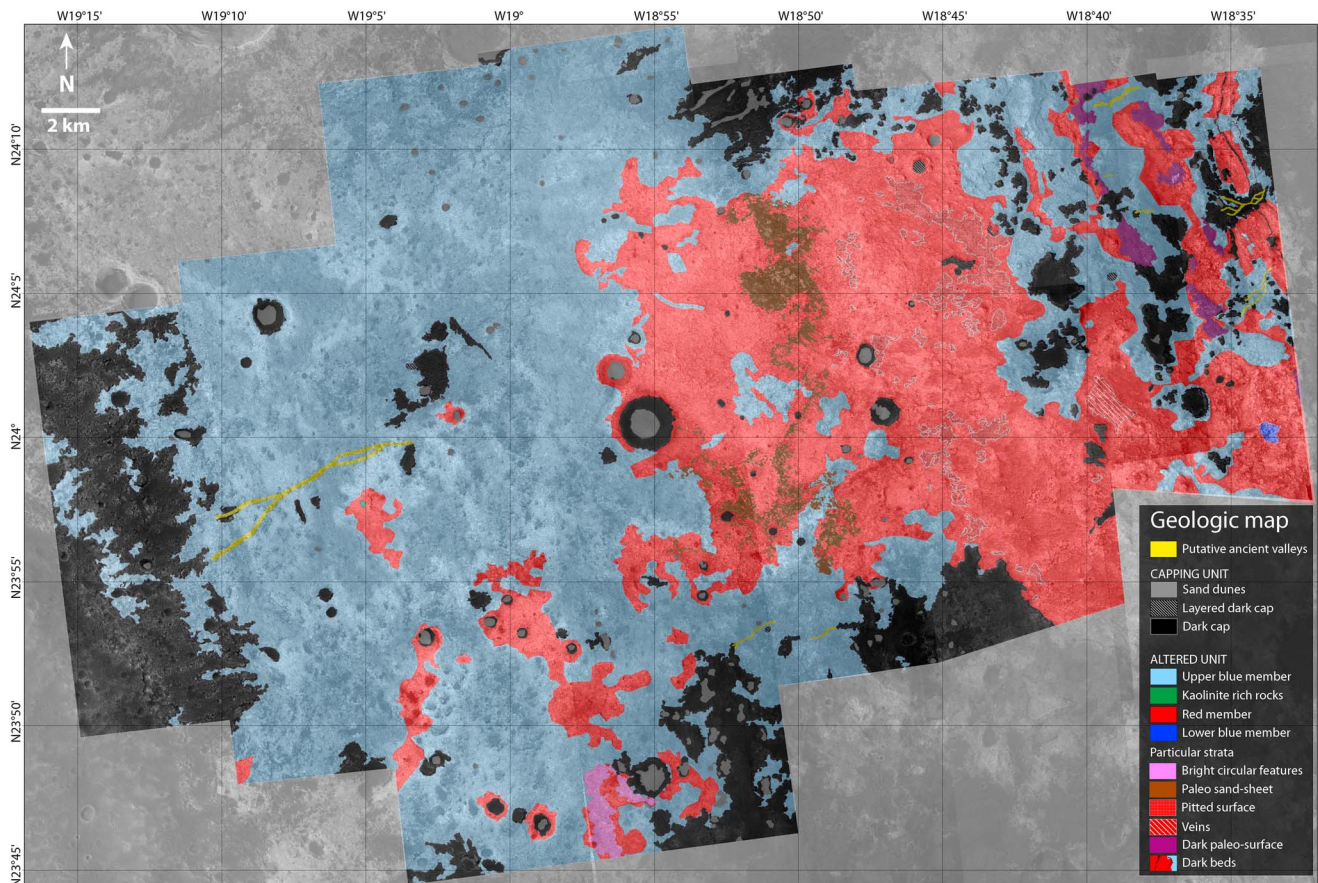


Figure 4. Geologic map (from Figure 3) of the study site superimposed on the HiRISE and CTX mosaic (from Figure 2).

Digital Terrain Models, DTMs, Figures 1 and 2b, calculated, respectively, by *Gwinner et al.* [2010] and *Gwinner et al.* [2015], based on stereo images from HRSC (High-Resolution Stereo Camera on board Mars Express [*Neukum et al.*, 2004]), and HiRISE DTMs provided by the HiRISE team also helped in calculating the thickness of the units. The flank of the Mawrth Vallis channel is clearly visible to the east and a part of the wall of Oyama crater to the west. The highest point corresponds to a 200 m high hill to the south. Another local high is located to the northwest. The rest of the plateau is relatively flat (450 m of difference in elevation from west to east for a distance of 30 km, 1.5% mean slope). A few eroded craters, < 2 km in diameter, are also visible.

We used the HiRISE mosaic as a base for the geological map. A CRISM mosaic (Figure 2c; modified from *Bishop et al.* [2013]) was also included in the mapping. The Al phyllosilicates and hydrated silica were mapped through the detection of an absorption band centered around 2.2 μm , Fe/Mg smectites through the detection of an absorption band centered around 2.3 μm , and an Fe^{2+} -bearing phase through the detection of a strong positive spectral slope from 1.2 to 1.8 μm [*Bishop et al.*, 2013].

One CRISM observation is also used to show spectral differences between geologic units. This targeted observation has been processed using the CRISM Analysis Toolkit (CAT, available and presented at <http://geo.pds.nasa.gov/missions/mro/crism.htm#Tools>) for the radiometric and atmospheric corrections. Spectra of regions of interest were ratioed by average spectra of surfaces with no hydrated signature within the same observation.

The HRSC false colors correlate well with the clay mineralogy such that Al phyllosilicates and hydrated silica detections from CRISM appear blue or white on the HRSC RGB mosaic (Figure 2d), while Fe smectites appear in tones of red, tan, pink, or brown [*Loizeau et al.*, 2010]. The same observation is made with HiRISE color images [*Loizeau et al.*, 2010; *McKeown et al.*, 2013], and some units are named by their false color appearance on the maps.

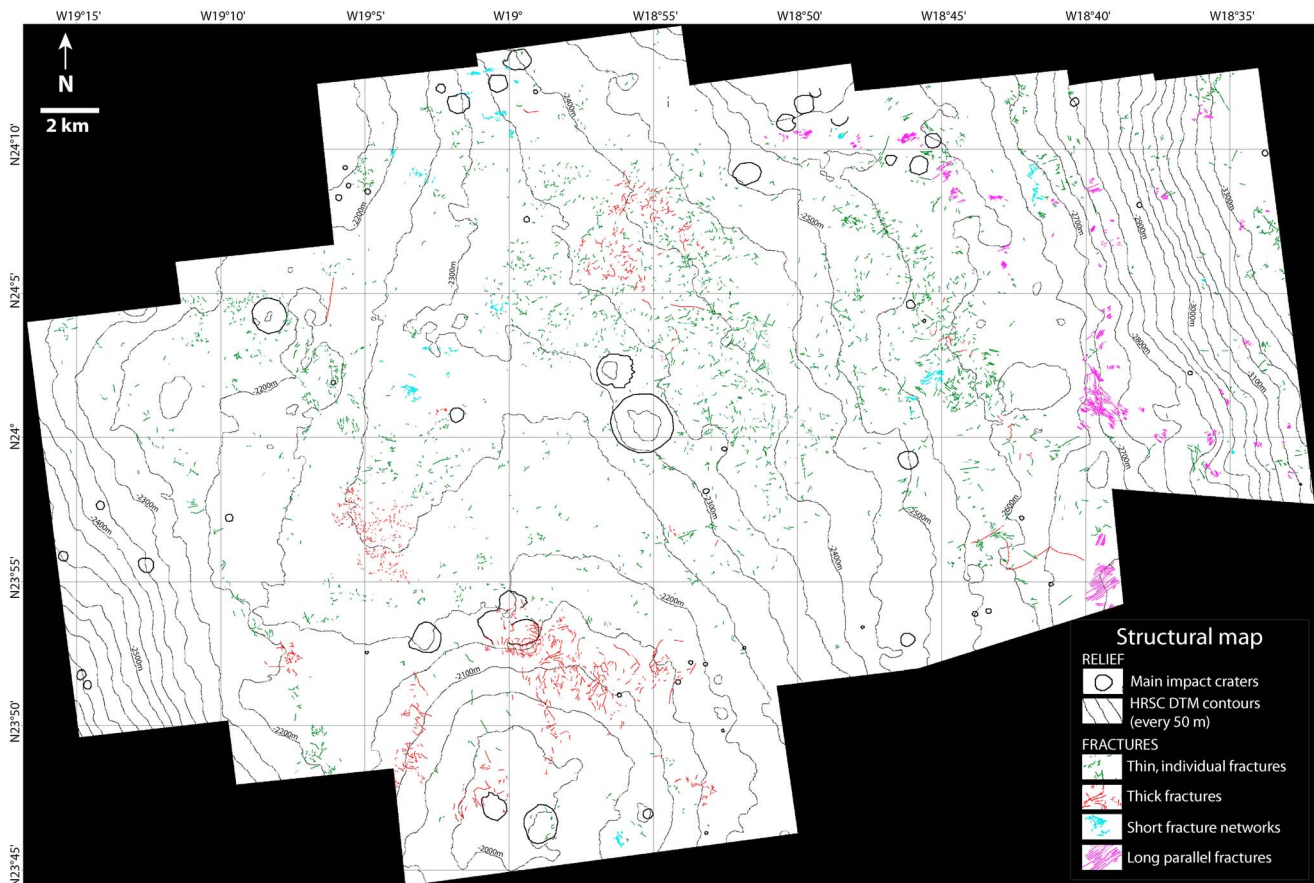


Figure 5. Structural map of the study site. The map displays the main impact craters and different kind of fractures, through their width, lengths, and organization.

2.2. Mapping Methods

Some morphological units can be identified directly with the greyscale images from HiRISE, such as the capping unit, possible ancient valleys and inverted valleys, or fractures. Mapping of the altered units required constant comparison between the CRISM mineral map, the HRSC RGB mosaic, and the HiRISE mosaic to follow the boundaries between the clay units and the correlation between the mineralogy, the color, and the morphology and texture of the rocks.

Two types of maps were prepared for the study site: a geologic map (Figure 3, superimposed on the CTX and HiRISE mosaic in Figure 4) and a structural map that shows in particular the main fractures (Figure 5, superimposed on the CTX and HiRISE mosaic in Figure 6). Close-up views of each unit and feature of the geologic map are described in the next section.

2.2.1. Geological Map

This mapping component of the study (Figures 3 and 4) involves identification and characterization of various geological units. We started by distinguishing two mineralogical units: stratigraphically at the top the “capping unit” shows spectrally no hydrated minerals; underneath, the lighter-toned “altered unit” exhibits multiple members with different hydrated minerals. Within the altered unit, particular strata, or group of strata, are identified through specific changes in albedo, morphology, and/or texture. Additional morphological features that cross cut the different units such as the “putative ancient valleys” are also mapped.

The capping unit contains the “dark cap” itself, local outcrops of “layered dark cap,” and fields of “sand dunes” on top.

We choose to distinguish members within the altered unit by compositional variations, which are consistent with the variations in color in the stretched color images. The “upper blue member” is composed of Al smectites, hydrated silica, and kaolinite, and an outcrop particularly rich in kaolinite: “Kaolinite-rich rocks” is also

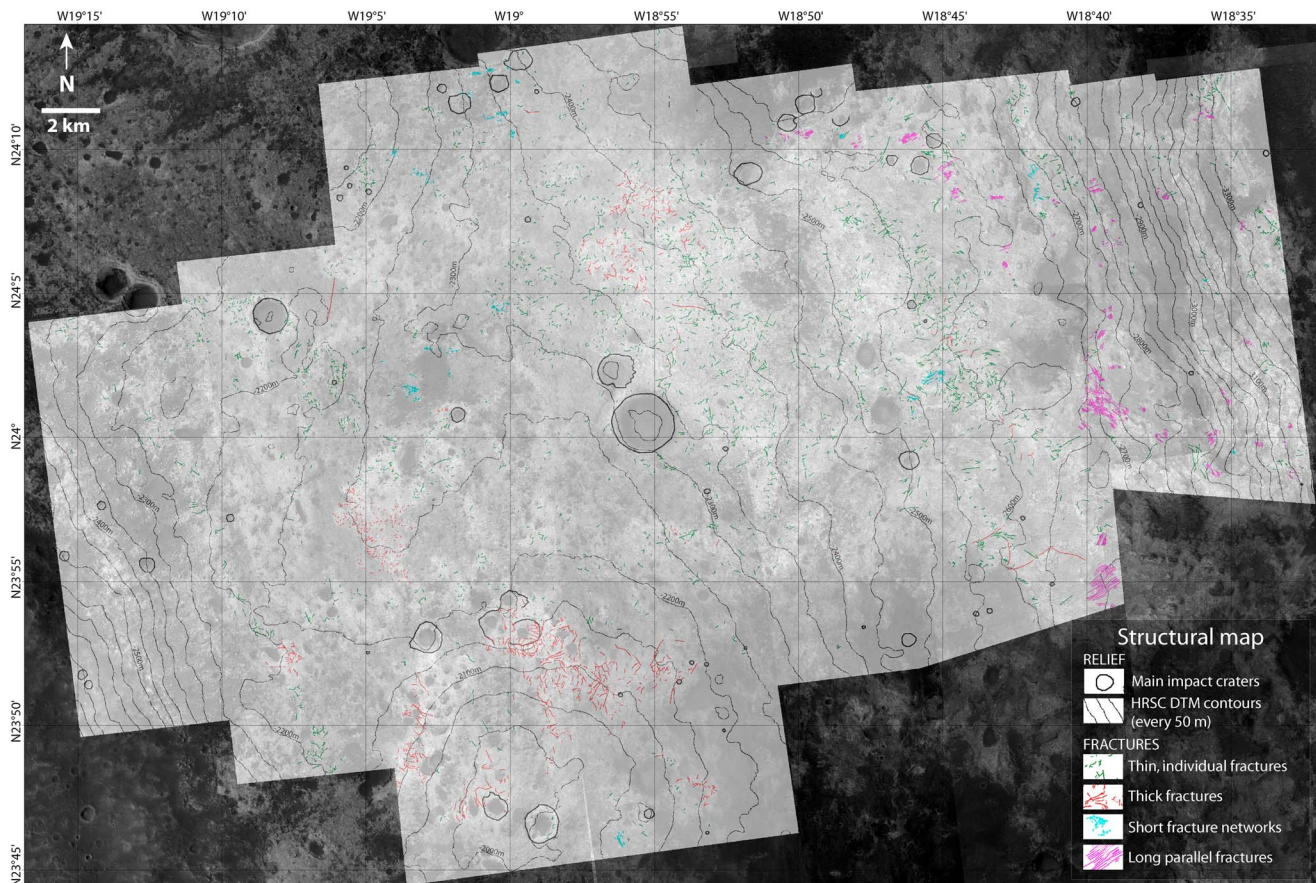


Figure 6. Structural map (from Figure 5) of the study site superimposed on the HiRISE and CTX mosaic (from Figure 2).

identified. The “red member” is composed of Fe smectites predominantly and lies below the upper blue member everywhere. The lower blue member is stratigraphically underneath the red member and appears blue in the stretched HRSC and HiRISE RGB images. However, its spectrum differs from these of the upper blue and red members, as shown in Figure 7. Within the same CRISM observation, when comparing spectral ratios of the different altered members, the lower blue member has an H₂O band centered at 1.93 μm but has a strong positive slope after 2 μm. It shows no absorption band around 2.2 or 2.3 μm and a very shallow inflection around 2.5 μm. This outcrop is lower on the flank of Mawrth Vallis and a higher density of aerosols there may make it more difficult to identify spectral signatures.

Particular strata, identified from a specific morphology, include the “bright circular features,” the “paleo sand sheet,” the “pitted surface,” the “veins,” the “dark paleosurface”, and the “dark beds.” They are mostly located within the red member, and they are detailed in section 3.

2.2.2. Structural Map

The structural map (Figures 5 and 6) shows the main crater rims and fractures identified in HiRISE images. When mapping the fractures throughout the study site, four types of fractures were identified: thin, individual fractures are visible throughout the site (many of them are represented in green, but some smaller ones are not mapped); thicker fractures (represented in red) are located in the Fe clay-rich rocks close to the Al clay-rich rocks; some local networks of short fractures are represented in blue; and other networks of long and thin parallel fractures are represented in pink. These fractures are further described in section 4 and displayed in Figure 12.

3. Detailed Characteristics

Table 1 presents the characteristics of the different geologic units mapped in Figure 3 and described in detail in this section.

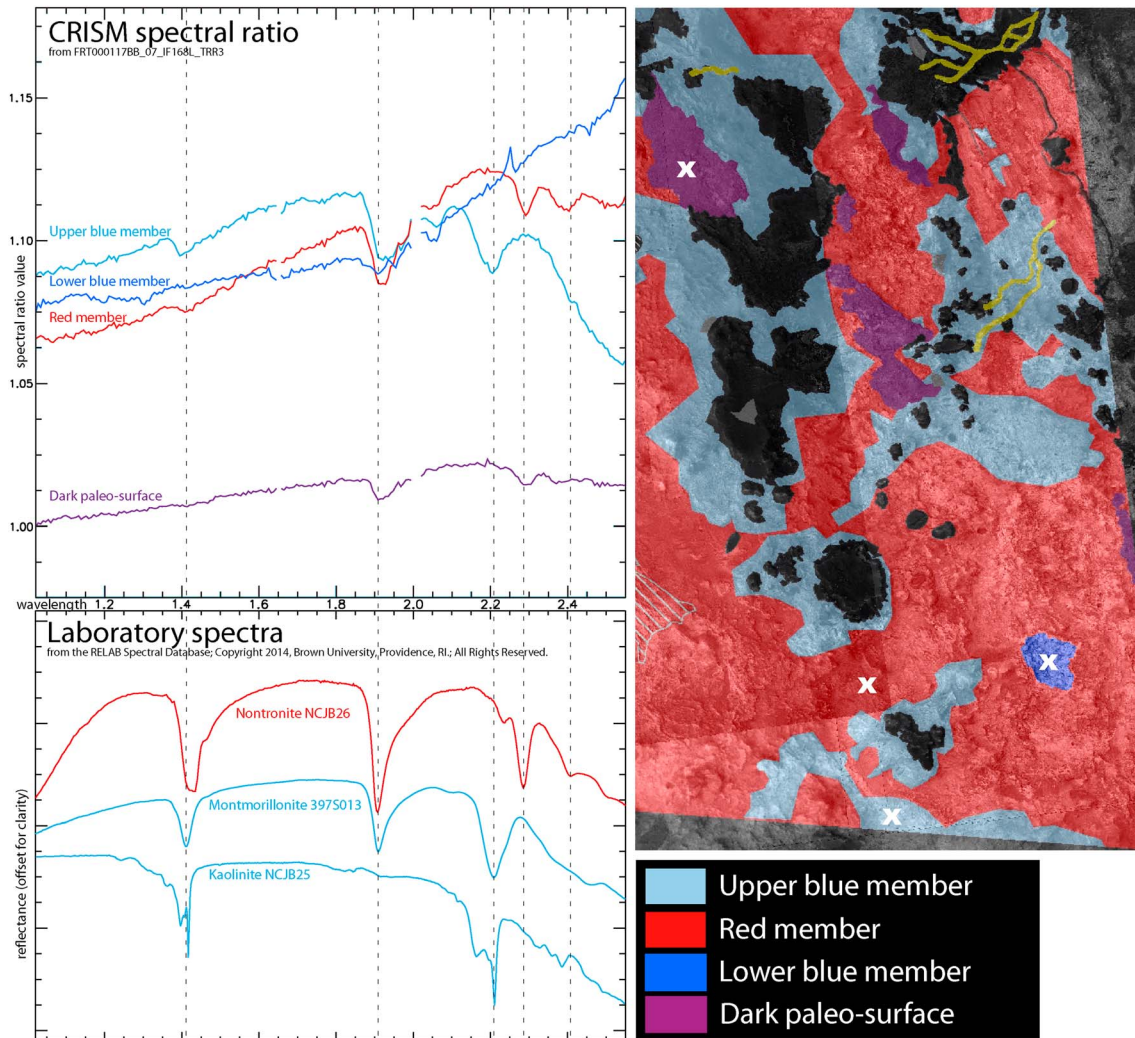


Figure 7. Spectra of the main units on the eastern side of the studied area and laboratory spectra for comparison. The white crosses indicate the positions of the 5 × 5 pixels areas where the average spectra were obtained. Some pikes were removed from the spectra, explaining the missing parts around 1.65 μm and 2.0 μm.

3.1. Capping Unit

The altered unit is partly covered by a thin dark cap (represented in black), sometimes layered (shown in dashed black), and by local dark sand dune fields (shown in grey), mostly on crater floors. Most small remains of the dark cap are located inside filled and eroded craters. Larger remains are located on each border of the mapped site.

We suggest that the dark cap unit once covered the whole region, before being partly eroded, as it homogeneously covers whole areas east and south of the clay-rich outcrops. It has a low thermal inertia (see Table 1) and hence would correspond to fine-grained material or poorly cemented rocks. It is generally about 5 m thick and not more than 10 m thick at the thickest points. Most likely, the deposits formed through air fall, which implicates either volcanogenic or impact-generated ash/dust [Noe Dobrea et al., 2010], and it has a weak signature of pyroxene [Loizeau et al., 2007]. It fills many ancient craters and is preferentially preserved there. It also forms isolated mesas in some locations (Figure 8c). These mesas are often surrounded by a dark talus material that also forms smaller cliffs at its base when eroded. We interpret these dark taluses to have formed with the erosional products of the dark cap rock; they were then indurated and then eroded again. Near and on top of the dark cap material are many small isolated dark dunes or ripples (they are few tens of meters long maximum). As these ripples are often located at the top of the mesas (Figures 8c, 8d, and 8f) and rarely found outside of the dark cap, we interpret them to be formed as erosional products of the dark cap rock and talus material.

Table 1. Characteristics of the Geologic Features Mapped in Figure 3 and Shown in Figures 7–10, in the Top to Bottom Order

Geologic Feature	HIRISE Stretched Color (IRB)	Morphology	Mineralogy	THEMIS-Derived Thermal Inertia ^a	Elevation Range ^b	Thickness ^c
Dunes	dark brown, brighter than dark cap	in local lows, generally ancient craters and valleys, direction: W-E in eastern part, SW-NE in western part	no hydrated signature, maybe basaltic sand if erosion product from the dark cap	135 to 180	full range: –1970 to –3400 m	highest dunes < 4 m high
Dark cap	dark brown, brighter on the edges of the cliffs	flat top mesas or crater filling, surrounded by dark talus; probably a “duricrust” protecting more easily erodible material	no hydrated signature, weak pyroxene signature [Loizeau et al., 2007]	180 to 325 (mostly 225 to 245)	full range: –1970 to –3400 m	2 to 10 m (mostly ~5 m)
Upper blue member	mostly dark to bright blue, sometimes light tan ^d	gentle slope forming unit, generally regular polygons 0.5–1.5 m across ^d	Al phyllosilicates (montmorillonite, kaolinite), hydrated silica, ferrous component at the contact with the red unit	180 to 290 (mostly 225 to 245)	full range: –1970 to –3400 m	20 to 40 m
Red member (above paleo-sand-sheet)	light tan, brighter than upper blue unit	generally irregular polygons 2–5 m across, with variation in fracture styles, few exposed layers ^d	Fe smectite, ferrous component at the contact with the upper blue unit	340 to 470 (mostly ~375)	–2000 to –2460 m	total red unit thickness > 140 m
Bright circular features	light tan, with darker sand	similar to red unit, but with many quasi-circular features 15–50 m across	Fe smectite	405 to 440	–2000 to –2070 m	no proper thickness
Paleo sand sheet	dark brown, redder than the dark cap	rough, linear features trending NW-SE (different direction than surface dunes) ^d	no hydrated signature	355 to 405 (mostly ~390)	–2250 to –2500 m	remaining ~1m sand sheet, remaining paleo-dunes 2.5 m high at maximum
Red member (on the plateau, below the paleo dunes)	light tan to darker tan where more eroded (due to sand and wider space between fractured blocks)	generally irregular polygons 2–5 m across, with variation in fracture styles, few exposed layers ^d , very eroded areas	Fe smectite	240 to 340 (mostly 275 to 310)	–2400 to –2660 m	total red unit thickness > 140 m
Red member (on Mawrth Vallis flank and floor)	light tan to darker tan	generally irregular polygons 2–5 m across, with variation in fracture styles ^d , with many exposed layers	Fe smectite	355 to 490	–2600 to –3380 m	total red unit thickness > 140 m
Lower blue member	bright, light blue	partly fractured in blocks up to 1.5 m across, exposed layers	possibly bassanite, or zeolite (spectrally close minerals when weak signal)	390 to 405	–3080 to –3120 m	?
Dark paleosurface	dark brown, slightly brighter than the dark cap	hummocky terrain with many quasi-circular features 10 to 100 m across, interpreted as exhumed filled craters	Fe smectites	420 to 495 (mostly ~440)	three apparent levels –2830 to –2900 m, –3000 to –3130 m, and –3175 to –3210 m	dark bed thickness on the order of 1 m

^afrom the qualitative thermal inertia map available at <http://astrogeology.usgs.gov/Projects/MSL/> [Ferguson et al., 2006].

^bfrom the HSC DTM.

^cfrom HIRISE DTMs.

^dMcKeown et al. [2013].

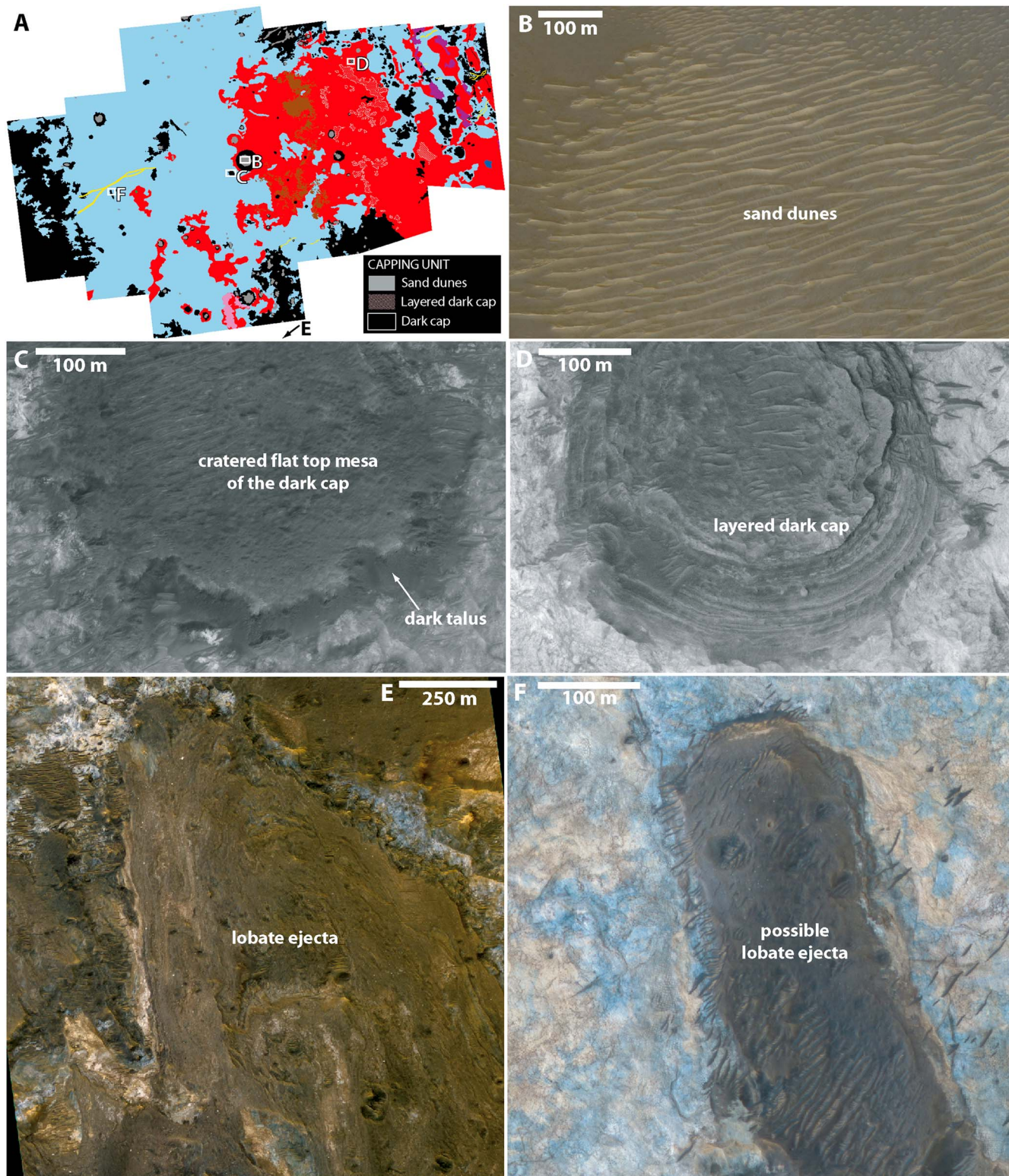


Figure 8. Different morphologies linked to the capping unit. (a) The location of the following HiRISE closeups on the geologic map. (b) Part of the largest dune field of the study site, in a crater. (c) Typical remnant mesa of the capping unit, with a cratered and hummocky surface and surrounded by a dark talus. (d) Some places, generally inside ancient craters, show this dark layered filling. (e) The capping unit mapped in the middle south of the study site may correspond to the lobate ejecta blanket of the crater (14 km in diameter) located to the south of the study site (visible in the closeup of Figure 1). This closeup is located 18 km from the center of the crater. Lobate linear features are visible, with many bright blocks or rocks mostly <1 m across. The largest exposed blocks are 5 m across. (f) Closeup on an elongated dark patch where bright blocks are also visible; their typical size is <1 m, and the largest are 2 m across. North is up for all images.

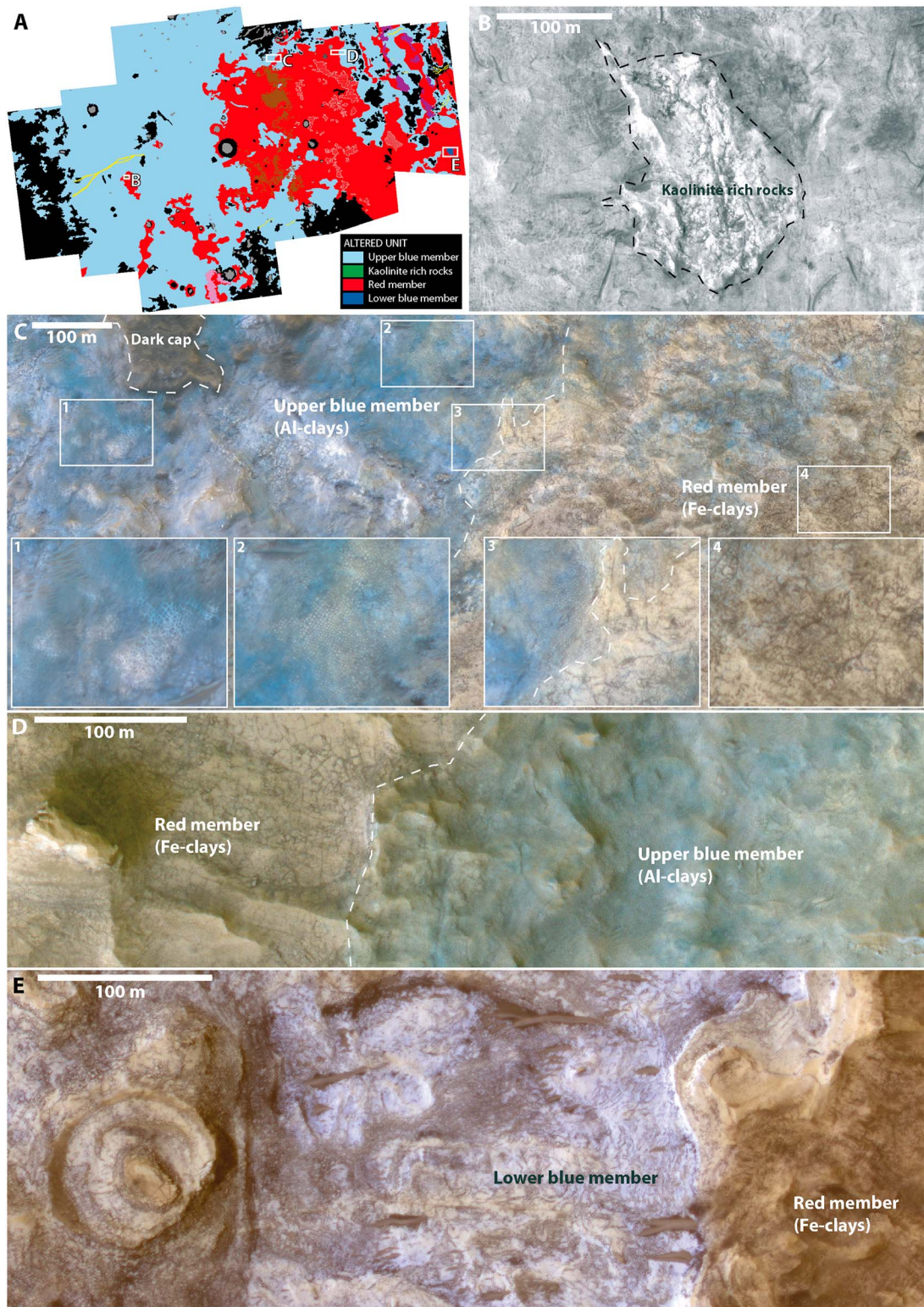


Figure 9. Different morphologies linked to alteration at the study site. (a) The location of the following HiRISE closeups on the geologic map. (b) Kaolinite-rich rocks corresponding to the brightest rocks of the study site. (c) Transition from the dark cap to the upper blue member and to the red member. Closeups (C1) to (C4) show the changing texture of the exposed units. (d) Transition from the upper blue member to the red member. (e) Closeup on the lower blue member. North is up for all images.

In some places, where the dark cap fills some holes (craters or ancient valleys [Michalski and Noe Dobrea, 2007]), the dark cap is layered (Figure 8d), while no layering is observed in most of its outcrops.

Small dune fields are located principally inside the eroded craters, on the top of the dark cap that fills most of them (Figure 8b). They have the lowest thermal inertia of the site, pointing to fine-grained sand, and their height does not exceed 4 m (Table 1). As they are often surrounded by the dark cap, we interpret them as originating from the erosion of the dark cap.

In addition, a 14 km diameter impact crater south of the study site is surrounded by a lobate ejecta blanket. The crater seems relatively recent as its ejecta blanket is still clearly visible and has been deposited on the floor of Mawrth Vallis. Also, the floor of the crater is only very slightly infilled by dune fields. Part of this thick ejecta reaches the southern side of the study site (Figure 8e) and shows lobate features and numerous small blocks of breccia. Further north, inside the studied site, a lobate form (Figure 8f) mapped as dark cap might be further ejecta remains of the same crater.

3.2. Altered Units

3.2.1. Main Units

Alteration on the plateaus around Mawrth Vallis created two main types of clay-rich units, the upper blue member and the red member. The contact between the two types of clays is generally more complex than what is mapped, especially in the center of the map: many small outcrops with Fe clays are located inside the blue part in the western half of the map. Also, Bishop *et al.* [2008] and McKeown *et al.* [2009] identified an additional spectral change at the contact between the Al clays/hydrated silica and the Fe clays, a strong positive slope from 1 to 2 μm attributed to an Fe^{2+} phase, with no particular difference in morphology or color from HiRISE data.

Alteration results in particular colors, morphologies, and textures in the high-resolution images in the visible domain [Loizeau *et al.*, 2010; McKeown *et al.*, 2013]. For instance, one particular outcrop, identified as particularly kaolinite rich, is very bright [McKeown *et al.*, 2013] and shows intense fracturing and appears more resistant than the Fe clay-rich rocks surrounding it (shown in white on the geologic map, around 19°05'W, 23°58'N, and in Figure 9b).

Figure 9c displays a transition between the upper blue member and the red member, with a small remnant of the dark cap in the upper left. It goes from left to right (from top to bottom) through the Al clay/hydrated silica-rich rocks of the upper blue unit: (1) Fractured, bluer rocks with bright fracture patterns and some sand cover; (2) with dark fractures, and through the Fe clay-rich rocks of the red member; (3) the boundary between the two members; (4) larger blocks of the redder fractured rocks, with dark fracture patterns. Blocks created at the surface by the fractures are regular and small (0.5–1.5 m across) in the upper blue member, while irregular and larger (usually 2–5 m across) in the red member [see also McKeown *et al.*, 2013]. More variability in fracture patterns is described in section 5. Figure 9d shows another transition between the two clay-rich units. Layers are present in the red member as seen around the butte in the region on the left. Dark sand is usually more common on the upper blue member than on the red member, and the surface of the upper blue member appears blurred there, possibly due to surface dust.

Another unit that appears as blue in the stretched HRSC and HiRISE color images is shown in Figure 9e. It is stratigraphically below the red member, located in a local low near the western margin of Mawrth Vallis, hence, called lower blue member. Its composition differs from that of the Al clay-rich rocks of the upper blue member, with hydration features (an absorption band centered around 1.9 μm is observed), but determining its composition is not possible due to the low quality of the spectral data resulting from high aerosol content in the atmosphere. Its morphology and HiRISE color are similar to the outcrops identified as rich in the Ca-sulfate bassanite by Wray *et al.* [2010]. In addition, smaller bassanite or analcime-bearing outcrops were identified nearby in small areas of the flank of Mawrth Vallis by Noe Dobrea *et al.* [2011]. They are not mapped here due to their small size (they only cover a few CRISM pixels, see Figures 12 and 13 in Noe Dobrea *et al.* [2011]). The very shallow inflection in the spectra around 2.5 μm (Figure 7) may correspond to the 2.5 μm band in the bassanite or analcime spectra.

3.2.2. Particular Strata

The layered red member displays several particular strata, revealed by the erosion from the top of the plateau to the floor of Mawrth Vallis. On the plateau, layers are close to horizontal, and as the terrain decreases in elevation from west to east across the study site, we explore deeper layers when going toward the east and the floor of Mawrth Vallis. However, on the floor of the Mawrth Vallis channel, layers dip toward the center of the

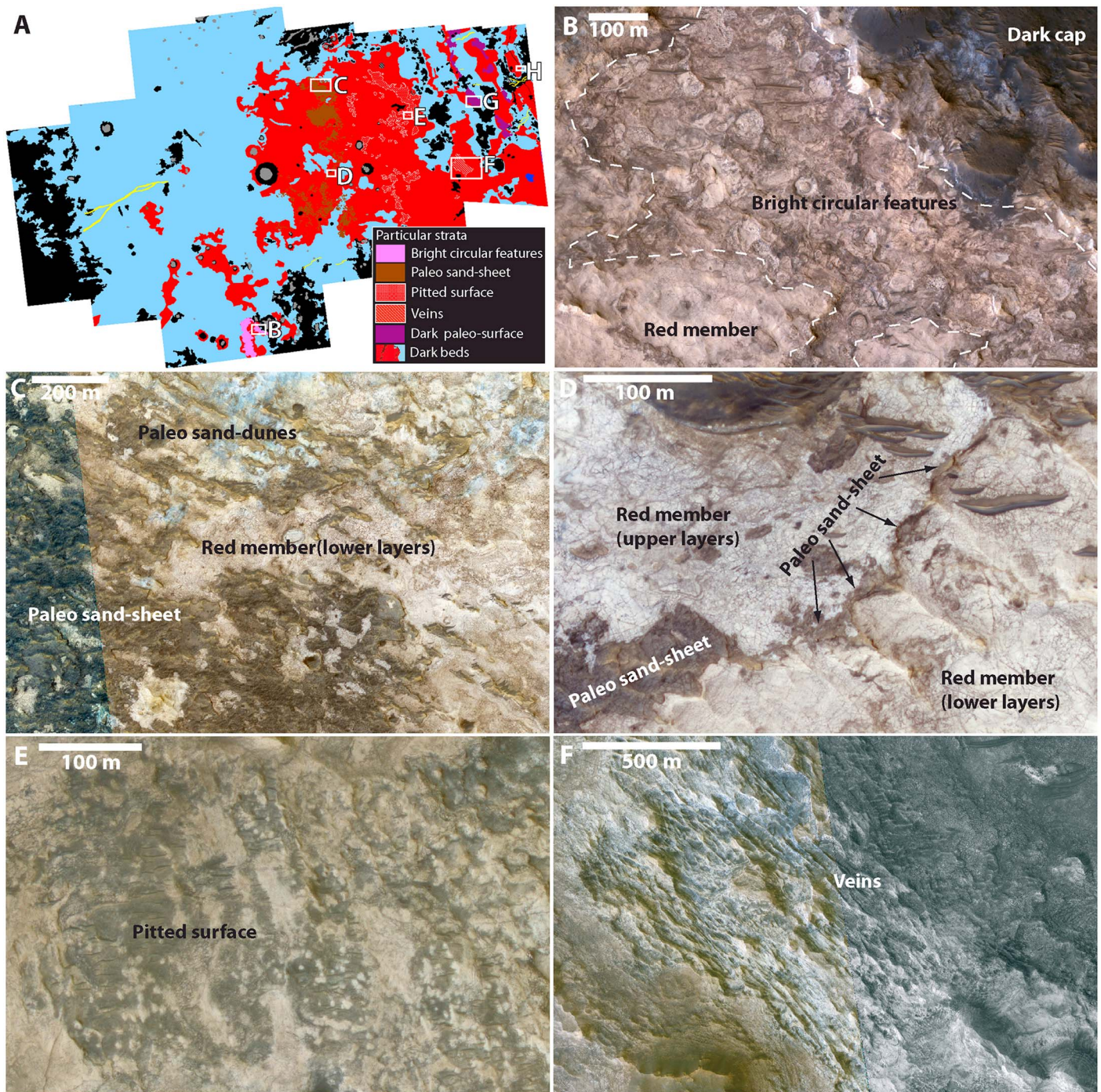


Figure 10. Different morphologies linked to deposition at the study site. (a) The location of the following HiRISE closeups on the geologic map. (b) This particular surface displays numerous quasi-circular features filled by the same material as the red member, interpreted as ancient filled craters, due to impacts before the deposition of the upper layers. (c) Rough, linear, dark brown features all trending NW-SE, interpreted as paleo sand dunes. (d) The paleo sand dunes and sand sheet seems sometimes to have been buried under upper layers; it may represent a hiatus in the deposition of the bright layers. (e) Pitted surface widely present in the eastern part of the study site. (f) Exceptional network of ridges, interpreted as veins, from inversion by erosion of mineralized fractures. (g) This dark Fe smectite-rich surface displays numerous quasi-circular features filled with slightly brighter material than the surrounding surface; the right image displays in white circles and ellipses these quasi-circular features. They are interpreted as ancient filled craters, due to impacts before the deposition of the upper layers. This surface is similar to the paleosurface described in Loizeau *et al.* [2010], Figures 8, 17, and 18. (h) The floor of Mawrth Vallis displays many individual layers with dips higher than the local slope. Some of those are indicated by white arrows. It also shows at least two dark beds, which can be followed over >10 km along the floor of the valley. North is up for all images.

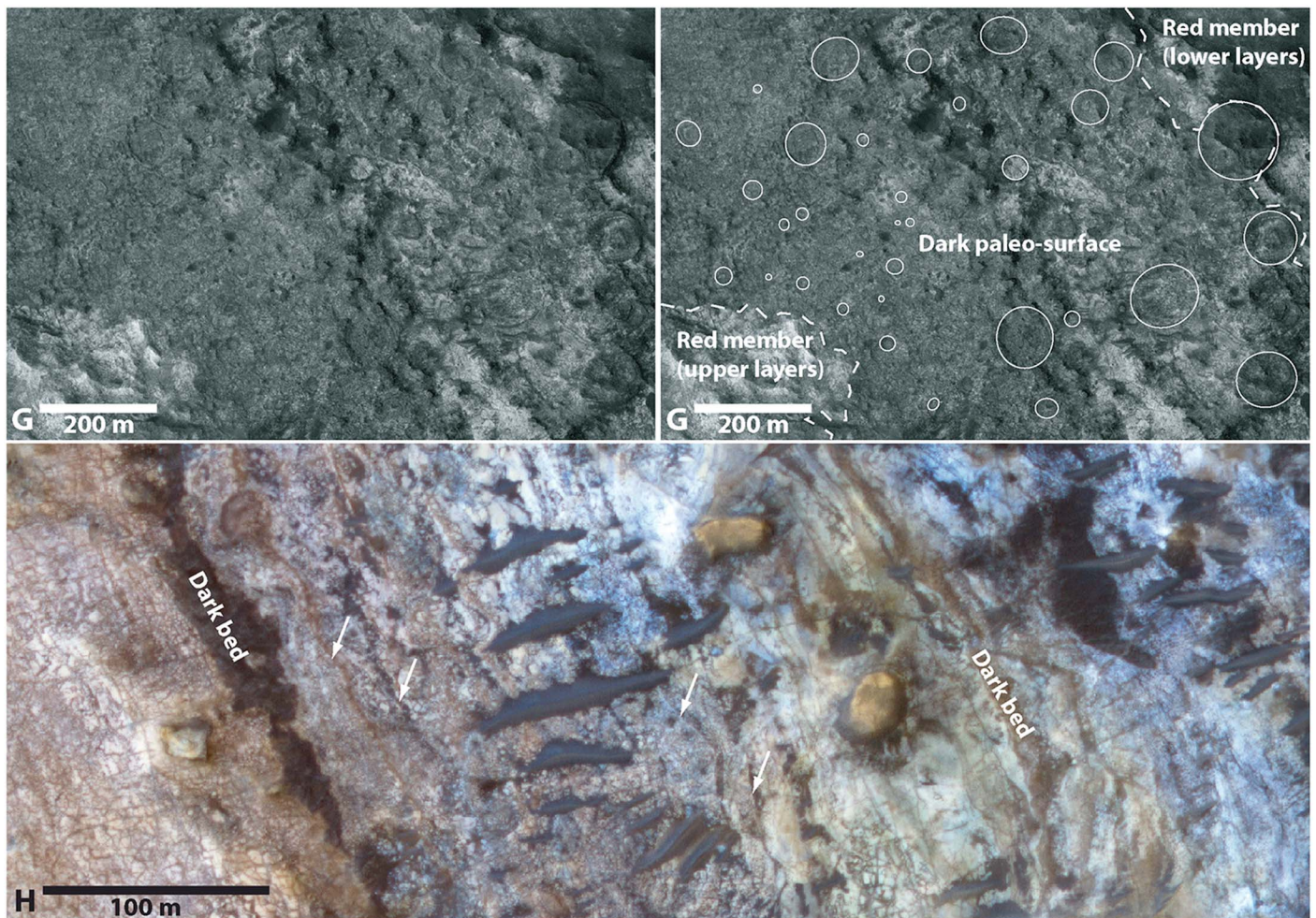


Figure 10. (continued)

Mawrth Vallis channel at a higher angle than the local slope [Loizeau *et al.*, 2012], which may indicate draping or mobilization after the formation of the channel itself. Due to the change in the dipping of the layers in that locality and the presence of numerous dark cap remnants, we could not make a continuous study of the layers on the flank of Mawrth Vallis.

In the south of the site lies a surface with numerous bright quasi-circular features (Figure 10b), 15–50 m in diameter. To first order, they look like features present in the dark paleosurface which were interpreted as ancient impact craters. However, these features are much more circular and have a much larger variety of sizes, while many of the bright ones are irregular in shape and the range of size is quite limited. Hence, we do not favor the hypothesis of ancient impact craters for those bright features. Rather, we attribute these structures as arising from the deposition of the layer(s) and their subsequent erosion.

From south to north in the middle of the site is mapped a dark layer (in brown on the map). It shows linear ridges oriented NW-SE (Figure 10c), which can be interpreted as a fossilized paleo sand dune field and sand sheet [McKeown *et al.*, 2013]. When looking at the western limit of this paleo sand sheet, the sand sheet appears as a dark bed in between an upper layer and a lower layer of clay-rich rocks (Figure 10d). Also, on the eastern side we see ridges in the same direction as the paleo dunes, indicating that paleo dunes were present at this very place but have been completely eroded away, while on the western side, no ridge is visible. Nevertheless, it is difficult to conclude if this paleo sand sheet is located in between two bright layers or if it formed after the erosion of the layered rocks; in this last case, the dark line in Figure 10d would just be a preserved external border of the paleo sand sheet.

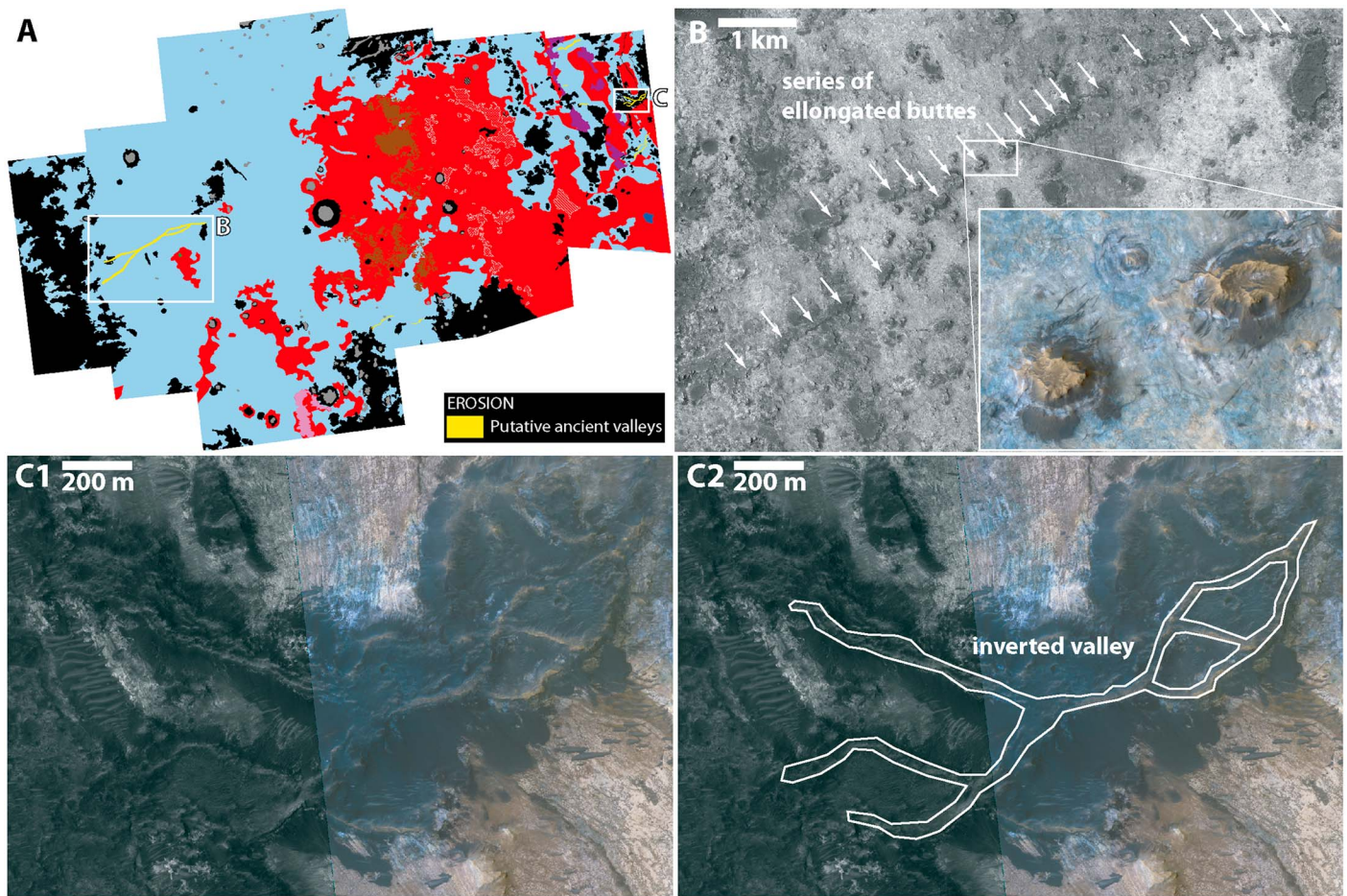


Figure 11. Different morphologies linked to erosion at the study site. (a) The location of the following HiRISE closeups on the geologic map. (b) Two series of elongated and quasi circular mesas joining together that may represent an eroded inverted valley. (c) Inverted valley and channel network on the flank and floor of Mawrth Vallis. North is up for all images.

Erosion also created particular landforms in the Fe clay-rich rocks in the eastern part of the site. In a few areas, we observe a pitted surface (as in Figure 10e). Pits are filled with darker material (probably dark sand) than the bedrock, and small irregular peaks are often present in the pits. They are the result of a more easily erodible layer than the rest of the red member, which was only present or only exhumed in this part of the site.

Near the flank of Mawrth Vallis, there are two sets of ridges intersecting at roughly 60° angles, leaving rhombohedral-shaped depressions between them (Figure 10f). We interpret these ridges as mineralized fractures that seem to correspond to a particular layer/set of layers inside the clay-rich rocks, where erosion excavated ancient sets of joints. A detail of this outcrop is displayed further in Figure 12k and discussed in section 4.

On the flank of the Mawrth Vallis channel, the other unit that has numerous quasi-circular features is much darker. It is mapped as the dark paleosurface (Figure 10g). It may be similar to the dark paleosurface identified in the western and northern parts of the Mawrth Vallis region [Poulet *et al.*, 2008; Loizeau *et al.*, 2010] but with smaller outcrops and smaller circular features. Also, the differences with the bright circular features of Figure 10b come from the larger variety in size of the dark paleosurface (from ~ 10 m to > 100 m in diameter in Figure 10g) and the presence of concentric features, while the bright circular features appear as plain discs, with cracks. This surface may represent a depositional hiatus, which recorded several impact craters and was subsequently covered by other layers.

On the floor of Mawrth Vallis, where layers are dipping at a higher angle than the slope [Loizeau *et al.*, 2012], some dark lines are observable over kilometers along the valley. We interpret them to be dark beds present between bright clay-rich layers. The outcrop of one of them (on the left side of Figure 10h) is particularly large

Table 2. Characteristics of the Fracture Types Mapped in Figures 4 and 5

Fracture Type	Location	Width	Length
Thin, individual fractures	on most clay-rich rocks surfaces	<1 m	~100 m
Thick fractures	in Fe clay-rich rocks, near the limit with Al clay-rich rocks	1–10 m	50 m to few km
Short fracture networks	in rocks just under the dark cap	up to 4 m	>100 m
Long parallel fractures	in Fe clay-rich rocks, in Mawrth Vallis flank	<1 m	>1 km

and is up to a few tens of meters wide. Another one is visible over a long distance (on the right side of Figure 10h) and can be followed over a few kilometers, while other thinner ones can be observed in a few places (arrows in Figure 10h) and can only be followed ~100 m). These thinner and shorter beds can be interpreted as deposits of dark sand, positioned in between bright altered layers.

4. Landforms Crossing the Main Units

4.1. Ancient Valleys

Valleys and inverted valleys are observed south and east of the study site, on the plateau, and on the Mawrth Vallis channel flank and floor (Figure 11). Inverted valleys (as in Figure 11c) appear where the surrounding dark cap has been eroded away but preserved inside the valley, revealing the ancient valley in positive relief.

There is also a 9 km long series of small, round, or elongated mesas in the western part of the site (Figure 11b). Each mesa is a few hundreds of meters long, > 15 m high, and comprised of clay-rich rocks that are covered by partially eroded dark material (~10 m thick at the top). Two series of these mesas, starting on the left, merge together toward the east and take a north-east direction. The series then bends toward the east and a smaller series of buttes just to the south of the main series seems to indicate a branching of this series of buttes. The elevation is the highest at the merging point and continues downslope both toward the east and the west. One hypothesis for its origin might be a crater chain that has been inverted through erosion of the clay-unit, but the merging of two series of buttes and the bending of the main series is difficult to reconcile with this hypothesis. It might otherwise represent an ancient inverted valley that has been deeply eroded, leaving the discontinuous buttes observed today (Figure 11b inset). However, the diverging slopes could refute this hypothesis, except if slope changes have occurred on the rim of Oyama crater on the western part of the series. We have mapped this feature as a possible inverted valley, although the morphology is not fully consistent with this interpretation.

4.2. Fractures

Most of the clay-rich rocks observed in this study are fractured at different scales. Table 2 presents a summary of the characteristics of the fracture patterns mapped in Figure 4. These features are described in more detail in this section and are highlighted in Figure 12.

At the highest HiRISE resolution, all clay-rich rocks are broken into blocks a few meters large at maximum (see Figure 9 in particular), as described in section 3.2.1 and in *McKeown et al.* [2013]. The small fractures dividing the rock into blocks are only present at the surface (not deeper than one or a few strata) and appeared and/or evolved only after the exhumation of the exposed layers. At depth, the fractures are probably present but closed, only millimeters thick and, once at the surface, cannot be seen at HiRISE scale before widening through erosion.

Small and thin fractures ~100 m in length and < 1 m in width are also present both in the upper blue and red members (for example, Figure 12b). They appear as individual fractures or joined with one or two other fractures at an angle $\geq 90^\circ$. They are mostly visible as dark lines, suggesting troughs filled by dark sand. Some of these fractures cross cut several clay-rich strata. This suggests that they could have formed before the exhumation of the exposed layers.

Larger fractures, a few meters wide and several hundreds of meters long, are present mostly in the upper portion of the red member, at the boundary with the upper blue member. Most have the same geometry as the smaller fractures (individual or joining with one or two other fractures at an angle $\geq 90^\circ$), but they often show bundles of fractures, with a primary large fracture surrounded by thinner parallel ones very close together. They are also probably filled by dark sand (typical example Figure 12c). In one area, around Figure 12d, the fractures are large, but particularly short in length (all < 100 m), and often surrounded by a bright halo.

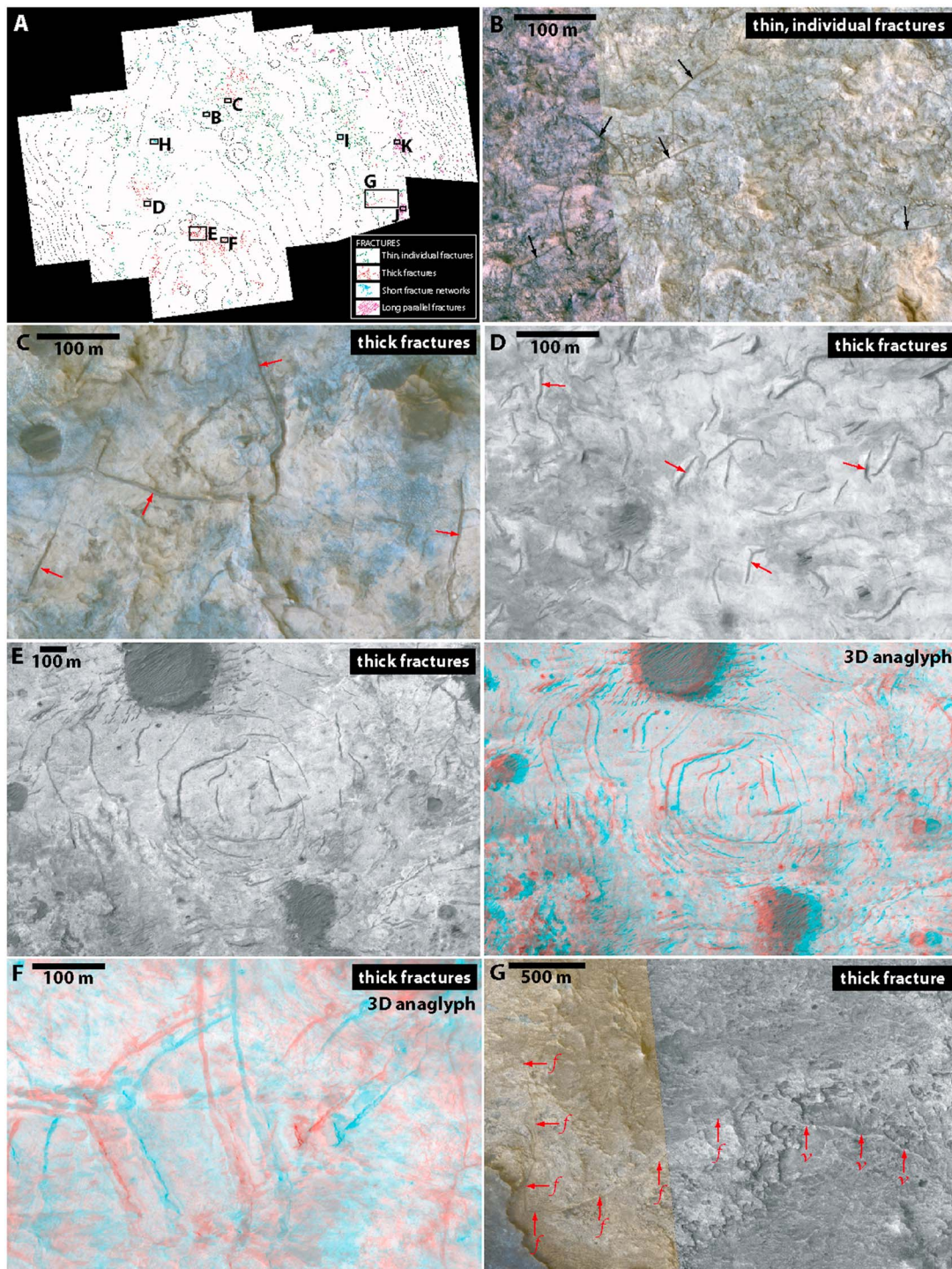


Figure 12. Different types of fractures at the study site. (a) The location of the following HiRISE closeups on the structural map. (b) Common, thin, individual, disoriented fractures, filled by dark material, present in both the upper blue unit and the red unit. Some of them are indicated by black arrows. (c) Thicker fractures, generally slightly sparser than the thin fractures, filled by dark material. Some of them are indicated by red arrows. (d) Thick and short fractures, often “halo bounded” (surrounded by a lighter zone); they are less connected than in Figure 12c and only occur in this area of the study site. Some of them are indicated by red arrows. (e) Thick fractures similar to Figure 12c but in a circular configuration. The anaglyph shows that there is no topographic sign of the circular feature. (f) Thick fractures similar to Figure 12c; sometimes partly in positive relief due to differential erosion. (g) Longest observed fracture (f) in the study site, forming an interpreted vein (v) toward the east. Fractures in Figures 12c–12g occur only in the red unit, generally close to the upper blue unit. (h and i) Complex network of thin to thick fractures, crossing each other in many different directions and delimited by blue dashed lines. (j) Large and dense network of thin fractures, mostly along two directions (pink arrows). (k) Network of thin dense fractures along one direction (pink arrow) and thin, more separated fractures (f) along another direction, partly forming interpreted veins (v), located in the zone of Figure 10f. North is up for all images.

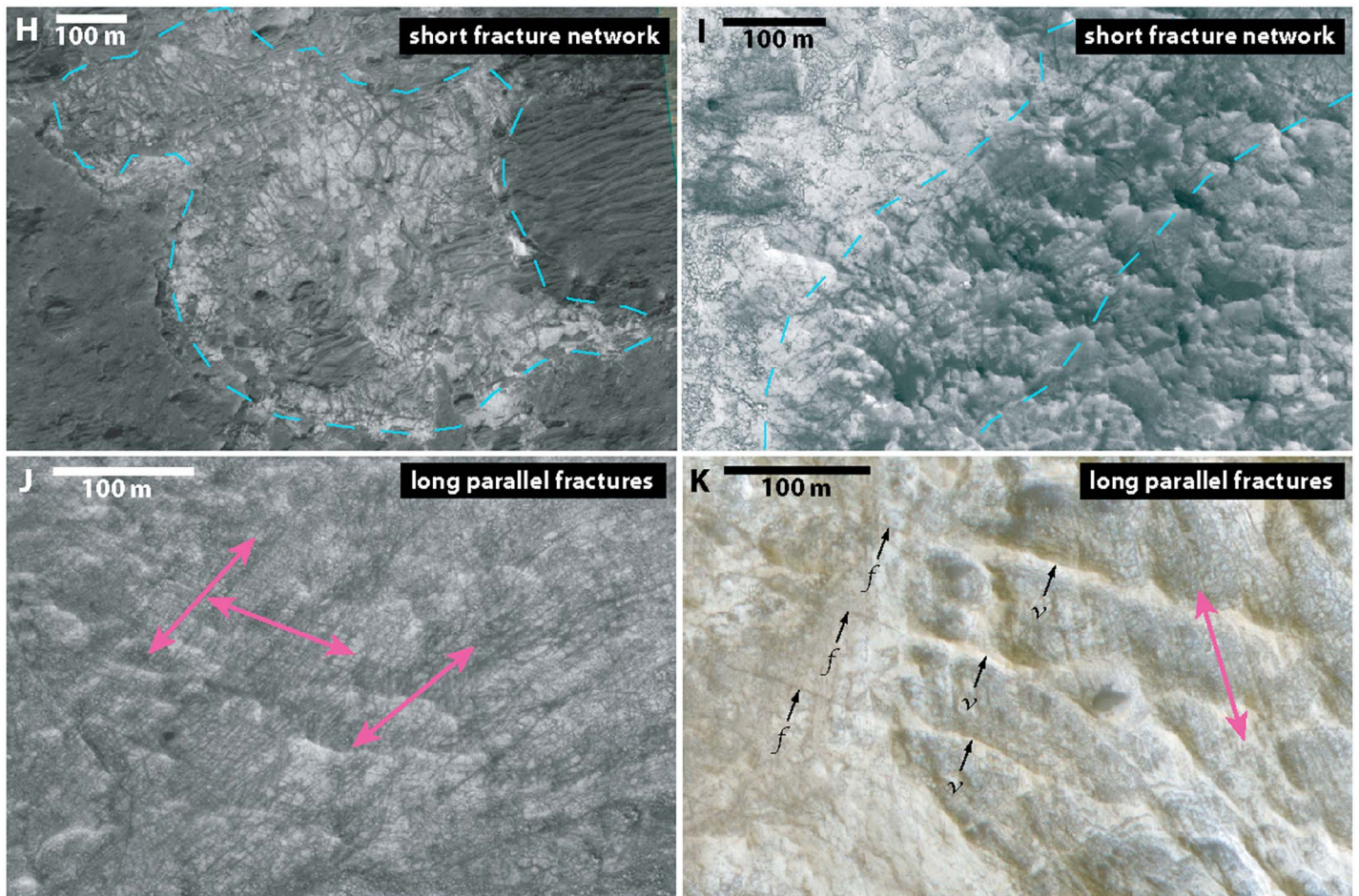


Figure 12. (continued)

Another particular set of fractures shows a concentric pattern (Figure 12e), not linked to the actual topography at this place (see the anaglyph). This suggests a local stress field. Some of these thick fractures, where the clay-rich rocks are strongly eroded, appear as what we interpret as veins in positive relief, and one fracture can extend from negative to positive relief across changing erosion patterns (for example, Figures 12f and 12g). In this case, the clay-rich rocks in close proximity to the dark fractures are preserved from erosion. Thin fractures are also evolving in interpreted veins in one area near the flank of Mawrth Vallis (Figure 12k). This phenomenon may be explained by fluid circulation inside the fractures, changing the physical properties of the clay-rich rocks around the fracture, as was hypothesized for the halo-bounded fractures in *Okubo and McEwen* [2007] in Candor Chasma and in Figure 6 from *Loizeau et al.* [2012] in another outcrop of the Mawrth Vallis region. Another hypothesis could be the formation of clastic dykes, due to the cementation of clasts inside ancient fractures.

Another type of fractures presents networks of relatively thick fractures that are a few hundreds of meters long at most (at least the visible part of them), located just underneath the dark cap (Figures 12h and 12i). These networks of fractures are not visible in the deeper layers and hence may be only surficial.

Larger networks are also observed near the deeper layers of the flank of the Mawrth Vallis channel. Those fractures are very thin (thickness not resolved with HiRISE) and long (>1 km). They are numerous (hundreds), parallel (in one to three different directions), and very dense, separated by < 3 m (see Figures 12j and 12k). We interpret them as the result of mechanical stresses in deep layers of the plateaus of Mawrth Vallis (they are approximately 700 m below the highest point of the study area). The impact that created the Oyama crater might be a source to these stresses.

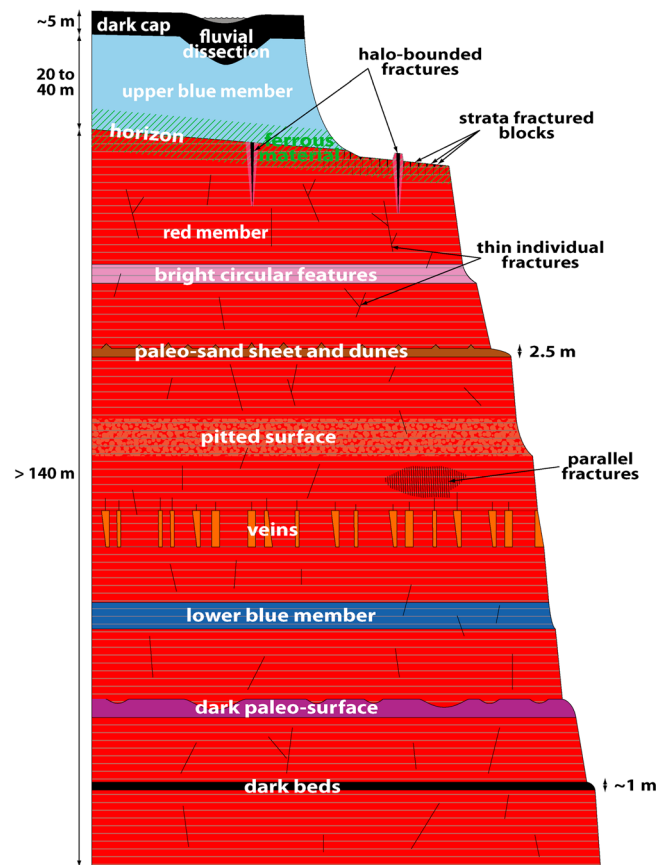


Figure 13. Schematic stratigraphic log of the first 200 m of the crust at the study site. The stratigraphic order is respected in the figure, at least from what is understood from the observations, but not the thicknesses of the particular strata, the space between them, and the size of the fractures.

5. Proposed Environments of Formation

Based on the geologic map, a schematic stratigraphic log is proposed (Figure 13), in order to help in visualizing the stratigraphic relationships between the different units and features described above. Note, however, that some stratigraphic positions, like the paleo sand sheet in between clay layers, are still only hypotheses.

This section first discusses the different hypotheses for the formation of the layered unit, the alteration, and the fractures. Then, a geologic history of the region is proposed, based on what we consider the most likely hypotheses.

5.1. Depositional Diversity

Geologic mapping reveals a variety of beds inside the thick clay-rich unit.

The red member shows light-toned layers, where the layering is mainly revealed within walls of craters on the plateau and in a few cliffs on the flank of the Mawrth Vallis channel. On the top of the plateau, the surface of strata is often exposed over large surfaces, and the transition from one stratum to another often shows many fractured blocks. The erosion on the top of the plateau often makes it difficult to track

the ends of the layers, as illustrated in Figure 14, as there is generally no visible dark layer between light-toned strata that could help to identify the border between strata. There are just a few dark beds, the most evident of which are found on the floor of the Mawrth Vallis channel, and as the Dark paleosurface and the paleo sand sheet on the plateau. It is also difficult to link the quasi-horizontal layers of the top of the plateau with the dipping layers on the floor of Mawrth Vallis [Loizeau *et al.*, 2012].

The process of deposition of the bright layers is difficult to determine as there is no obvious facies which could indicate a single process as pyroclastic or aeolian deposition, or fluvio-lacustrine sedimentation.

The diversity of the observed deposited layers enables us to derive several distinct environments. The presence of other types of layers (like the dark beds, the dark paleosurfaces, and the paleo sand sheet) in between light-toned clay-rich layers illustrates hiatuses in the clay depositional environment.

Dark beds as seen on the floor of the Mawrth Vallis channel (Figure 10h) point to the deposition of a different material, less altered than the light-toned layers. For example, thick deposits of pyroclastic material such as ash distributed under dryer conditions may form such darker layers, but it could also indicate a different source of sediments or wind deposits such as basaltic sand. The proposed dark paleosurface (Figure 10g) also points to an interruption in the deposition of the plateau layered unit, as it is located between two sequences of clay-rich layers. The proposed paleo dune field (Figures 10c and 10d) also shows the passing of a sand field moved by wind. The question of its presence in between clay-rich layers or after the erosion of the clay-rich layers would give more precision to the chronology: if it is located between clay-rich layers, it would indicate a dry episode during the deposition of the clay-layered unit. If it is not between them, then the sand field passage would have occurred much later, after the erosion of the altered unit.

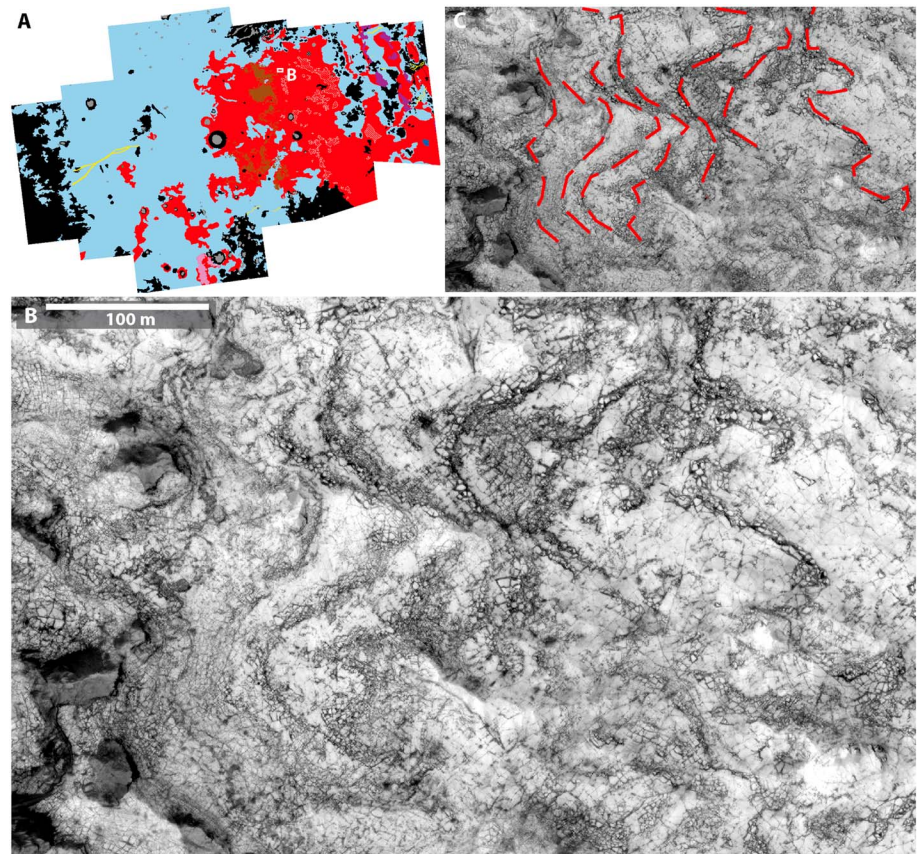


Figure 14. Example of clay-rich layers' limits. (a) Shows the location of the following HiRISE closeup on the geologic map, near the paleo sand sheet. (b) HiRISE closeup on an outcrop of Fe clay-rich layered rocks. The general slope goes down from left to right. Illumination comes from the lower-left. An interpretive map of the limit of seven layers is shown in red in Figure 14c on the same image. We see successive fractured strata; their external limit are more fractured, and blocks are separated. The space between blocks is filled with darker sand or dust, making the limit of layers appears darker. When the erosion is more progressive, the limit from one stratum to the other is less visible as on the lower part of the image. North is up for all images.

Differences also appear between clay-rich layers of apparent similar color and composition given by visible and near-IR reflectance. In this case, the differences in physical properties (compaction, grain size, or some mineralogical mixtures) that lead to the observed different morphologies are not revealed by the nadir spectra. For example, the pitted surfaces near the flank of Mawrth Vallis show that some layers of the Red member have different responses to erosion than others. A weaker compaction of this layer or the presence of soluble minerals may explain these pits but an in situ study would be needed to discriminate the origin of this difference. The bright circular features are another example where response to erosion reveals a different layer.

The dark cap (Figure 8) shows the end of the deposition of clay-rich material and of the surface alteration in the region. This dark cap is very widespread in the Mawrth Vallis region and is observed at the surface of many regions where clays were identified [Ehlmann *et al.*, 2011; Carter *et al.*, 2015]. It forms at Mawrth Vallis as large flat outcrops where crater counting can be performed. It may constitute a good candidate for returned samples to be dated for comparison with crater retention ages. The layering observed in some parts of the capping unit may be due to remobilization and sedimentation of the dark cap material, indicating that it would have been reworked since its initial deposition, by wind for example. The surface has also been locally covered by impact ejecta, especially from the fresh 14 km large crater south of the study site.

5.2. Alteration Environments

Fe clay-rich layers are observed over a thickness > 140 m at the study site, as revealed on the flank of several eroded craters [Loizeau *et al.*, 2007]. Heterogeneity between layers of the red member is revealed by dark beds and more erodible layers, but IR spectra show a similar composition over the whole section, and color

variation of clean light-toned layers is very limited, except toward the top of the section, near the upper blue member [Bishop *et al.*, 2008; McKeown *et al.*, 2009]. This homogeneity points to an overall stable alteration environment during the deposition of the entire red member. Layers could have formed directly as clay-rich, fine-grained detrital products of an altered bedrock in a fluviolacustrine context or as the progressive authigenic alteration of fine-grained deposits (dust, ash or silt) from pyroclastic, aeolian, or fluviolacustrine deposition (e.g., Loizeau *et al.* [2007] or Bishop *et al.* [2008]), forming a paleosol sequence as proposed by Horgan *et al.* [2013], or possibly to a homogeneous alteration of the whole section after its deposition. However, the large thickness of the section makes this last hypothesis less likely.

The top of the section, the upper blue member, shows a different composition with Al clay/hydrated silica-rich rocks, consistent with a late downward weathering of the rocks by surface water [e.g., Loizeau *et al.*, 2012], or the deposition and alteration of basaltic material in slightly acidic waters or a change in composition to more silica-rich ash [Bishop *et al.*, 2013]. Michalski *et al.* [2013] propose a formation by alteration of dust or ash by acidic snow and ice deposits that could account for the top-down nature of the alteration, the fine-grained nature of the deposits, and the diffuse contacts between altered strata, without requiring significant amounts of chemical erosion. Moreover, Al clay-rich rocks are not limited to one layer or on top of a particular layer, but cross-cut strata, are present over different altitude levels and appear to drape over the red member, with a stratigraphic limit analogue to a leaching horizon, consistent with a formation at the surface, after the erosion of the previously deposited layers. For example, the incision of the Mawrth Vallis channel should have happened before the formation of the Al clay-rich rock, as those are present on the flank and near the floor of the outflow channel. The presence at the top of the section of different Al clay minerals (kaolinite and montmorillonite) or hydrated silica, sometimes spatially separated, also shows a very large variety of environments in this unit, either in terms of parent rock or fluid circulation and chemistry. Were the layers already rich in Fe clays before the formation of the Al clays? This is probable given the thickness of the layered Fe clays (>140 m). In this case, the formation of the clay sequence would be different than that of a single pedogenic alteration as identified in thinner clay sequences on the plateaus surrounding eastern Valles Marineris [Le Deit *et al.*, 2012], in Nili Fossae [Gaudin *et al.*, 2011], or in a few other regions of Mars [Carter *et al.*, 2015]. Here the pedogenic alteration built on preexisting smectite-rich deposits rather than on mafic bedrock.

The lower blue unit has a similar morphology and HiRISE stretched color than Ca-sulfate-rich outcrops identified in the vicinity in local lows, on the floor of Mawrth Vallis by Wray *et al.* [2010], although the available spectra could not help determine its composition. The possible presence of Ca-sulfate shows an even greater spatial variety of environments within the study site with the possible precipitation of sulfates in the deep section, as byproducts of the alteration of the upper layers for example.

5.3. Tectonic History

The site also shows a variety of fracture patterns. Beside the surficial fracturing of the exposed layers due to their contact with the atmosphere (contraction due to desiccation or temperature variations [Loizeau *et al.*, 2007; McKeown *et al.*, 2013; El-Maarry *et al.*, 2014]), longer fractures are found in many clay-rich layers of the site. In particular dense fracture patterns are observed in the deeper layers of the red member, on the flank of the Mawrth Vallis channel (mapped in pink in Figure 4 and in Figures 12j and 12k). They reveal higher mechanical stresses in these layers, maybe linked to the impact that formed the nearby Oyama crater.

5.4. Surface and Subsurface Fluids Flow

Ancient valleys and inverted valleys are located primarily on the flank of the Mawrth Vallis channel but also on the plateau. They show fluvial activity at the end of the deposition period and alteration of the entire clay-rich unit. Fluids also circulated inside fractures in the subsurface of the plateau. They precipitated minerals and indurated material inside fractures and in the rocks close to the fractures through circulation in the porous space of the rocks, forming halo-bounded fractures, in particular for the fractures close to the interface between the red and upper blue members. The same observation has been made in another part of the same region [Loizeau *et al.*, 2012] and elsewhere on Mars [Okubo and McEwen, 2007]. The densest set of veins is observed on the flank of Mawrth Vallis, in deeper layers. This may be explained by the presence of an ancient aquifer circulating at this level in the ancient subsurface. This indicates that fluid circulation was still happening, at least in the subsurface, after the formation of the fractures, thus well after the cementation of the layers.

5.5. Geologic History

The proposed geologic history discussed in this section favors some of the hypotheses presented above and in the literature on the Mawrth Vallis region. It is therefore not unique, but we consider it as the most likely given our knowledge and our understanding of the geologic events that formed and shaped the outcrops in the Mawrth Vallis region.

Deposition of the Fe smectite-rich red member began early in the Martian history, possibly in the Early Noachian [Loizeau *et al.*, 2012], in a wide-spread low-lying region of Arabia Terra near Chryse Planitia, under a wet environment. The transformation of this expansive deposit into the observed mudstone in surface or near-surface conditions (diagenesis) would have required sustained water activity even in the case of dust deposition.

Tectonic activity may have occurred about the same time as clay formation. The outflow channel takes two 90° turns, and the layers dip at a different angle on the floor of Mawrth Vallis [Loizeau *et al.*, 2012]. This could be explained by tectonic activity creating a valley where Mawrth Vallis is visible today. At least one hiatus in the deposition created the dark paleosurface which recorded impacts, creating craters that were then buried under later units. Some dark beds also show rapid deposition of other types of sediments (such as coarser sand deposits).

Much of the red unit was deposited when a large impact created Oyama crater, likely fracturing heavily what are today the deepest visible layers of the red unit. Erosion probably removed and transported away most of the ejecta from Oyama, which is not clearly visible today.

During the Late Noachian, the outflow of waters across Mawrth Vallis to the northern lowlands carved the region that is now the large valley at the east of the study site.

A last episode of hydrous activity at the surface eroded the rim of Oyama, transporting clay-rich material and depositing it on the floor of Oyama. We interpret that this event intensively leached the surface of the red member, creating the upper blue member by further alteration of the smectite-rich layers and also eroding several small valleys on the plateau toward Oyama, Mawrth Vallis, and the northern part of the region. Percolating fluids inside fractures of the red member also modified the rocks at the contact of these fractures and precipitated minerals inside these fractures.

Large volcanic events on the planet in the Early Hesperian deposited the dark cap, a few meters thick layer of pyroclastic material across the whole area, covering the upper blue unit.

After this episode, impact craters and wind erosion slowly eroded the dark cap, remobilizing its material to create patches of layered dark cap and sand dunes and revealing portions of the Altered unit underneath. This erosion opened windows through the upper blue member to much deeper layers in the red member. Inverted valleys and veins were raised by differential erosion. The remaining parts of the dark cap appear as mesas on top of the hydrated units.

6. Preservation of Potential Biosignatures

A critical point for a mission seeking biosignatures is preservation of the ancient environments and the potential biosignatures: this requires, in particular, (i) no deep burial of the rocks and (ii) fresh outcrops that have not been exposed to the dry atmosphere, oxidation, or cosmic rays for long periods of time.

The presence of smectites in the rocks shows that they were not exposed to high temperature and pressure. In particular, the Al clays formed at or very close to the surface (as a draping unit over the Fe clay-rich layers), and there is no sign of burial of those Al clays, except for the <10 m thick dark cap rock.

In addition, very few recent craters are observed on the clay-rich outcrops, pointing to relatively recent exposure of the rocks. First, the surface has been covered by the capping unit for part of the time, providing protection for the clay-rich rocks, and second, the relative softness of the clays can explain why the rocks are readily eroded, rapidly providing fresh outcrops. It may be possible to locate the freshest surfaces through further analysis.

To evaluate the freshness of the clay-rich outcrops and the rate of erosion of the surface today, we estimated the impact cratering retention age of the clay-rich rocks. We focused our crater counting on the red member of the study site, as delimited in Figure 15. No fresh impact craters are observed, making the crater count itself difficult for crater diameters below 25 m as all small impact craters are very much eroded. Under this value,

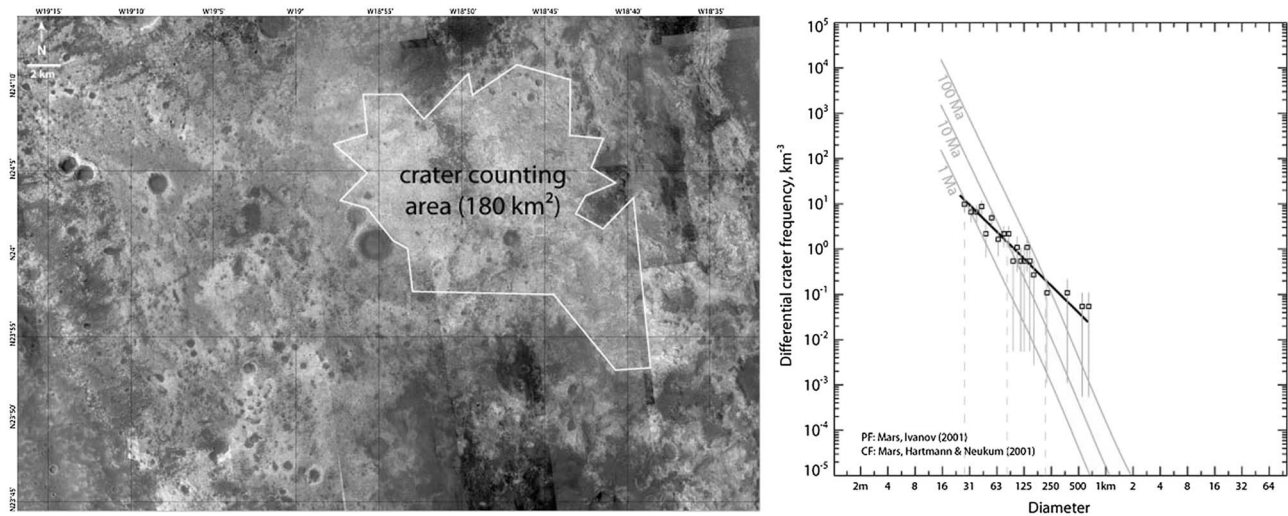


Figure 15. Evaluation of the exposure of the clay-rich rocks. (left) The HiRISE mosaic with the crater counting area delimited in white; (right) The crater distribution compared with isochrones at 1, 10, and 100 Ma.

we can barely discriminate impact craters and hollows created by simple erosion of the clay-rich unit. Typically, for small impact craters we detect only dark circular deposits in the depression but no clear crater rim. Only 64 impact craters were counted in the 180 km² area, with diameters between 25 and 660 m.

We have used the “craterstats2” software developed and described by *Michael and Neukum* [2010] to compare the measured crater size-frequency distribution. We used the crater production functions derived from *Ivanov* [2001] and the chronology function from *Hartmann and Neukum* [2001]. The crater frequency distribution crosscuts isochrons as the surface is continuously eroded. Smaller craters are erased more rapidly than bigger craters; hence, the retention age for smaller craters appears younger than that for bigger craters.

From the crater size-frequency distribution that we measured, no isochron is followed, even for the larger diameters, making it impossible to determine the age of the start of the exhumation, but we can deduce that the erosion of the clay-rich unit began at this location more than 100 Ma ago (possibly more than 1 Ga ago) and does not appear to have stopped since then.

Although the erosion seems to be continuous across the study site, it is not uniform on the terrain, due to the layered nature of the rocks. We would increase even more our chances of finding fresh outcrops, and hence potential biosignatures, when searching in scarps, or at the limit of erosion of strata: the layer below the eroded one would have been protected until recently by the layer above.

7. Possible Targets and Traverse for an IN SITU Mission

To maximize the scientific return of a rover mission, a high diversity of geological targets is required, in addition to the general habitability potential of the site. The study site offers a high variety of targets, in terms of deposition, alteration, erosion, and transport as described in the previous sections. Several potential targets were previously proposed within and near the landing ellipse defined for MSL [*Mangold et al.*, 2011].

The few strongly eroded impact craters at the study site would be valuable targets to investigate the physical and mineralogical stratigraphy. Within a short distance, these craters would provide access to materials deposited over a long time period and formed under multiple geochemical environments. In addition to this variety, the slope of the crater walls provides more efficient erosion than that of the intercrater area and hence fresher outcrops. However, these crater walls are not steep, and it has been shown that any crater at the site would be escapable by a rover like Curiosity [*Golombek*, 2011].

The transition from the upper blue member to the red member is also a priority target. The border between the two types of clays is present in many locations of the study site; thus, wherever the rover lands, only a short drive would be required to access this geochemical boundary. It has been proposed [*Bishop et al.*, 2013] that this transition could be a relic of particular chemical or biological redox reactions. Also, it would

be crucial for the understanding of the geologic history of the region to determine if the parent rocks prior to alteration were the same for both units.

The valleys and inverted valleys of the site would also constitute priority targets, in order to study the deposits at the base of their floor. The floors are filled by the capping unit deposits, but the sides of inverted valleys enable access to the deposits. These deposits could host rapidly buried molecules, the identification of which is an objective of the Mars 2020 mission.

Fractures offer other targets; in particular, the inverted fractures and halo-bounded fractures could point to fluid circulation in the fractures. These rocks could provide additional context where possible life could have been preserved, and in situ analysis would provide additional information on the chemical history of the region after the deposition of the layers.

Also, sampling the capping unit, preferentially the nonmodified dark cap, would provide a way to study volcanic material (ashes and other pyroclastic deposits) that has not been analyzed previously and determine an isotopic age for this unit that could be linked to its crater retention age [Loizeau *et al.*, 2012].

A possible traverse would extend mainly on a west-east axis. It would provide the opportunity to (i) investigate the Al/Fe clays transition, (ii) analyze many unique strata exhibiting multiple physical properties (the clay-rich strata, the paleo dune field, the paleosurfaces, the pitted Fe clay-rich strata, and the dark beds), (iii) examine outcrops of unique mineralogy such as the kaolinite-rich outcrops and the lower-blue unit, (iv) inspect different types of fractures and more importantly some that experienced fluid circulation, and (v) probe ancient valleys. Additionally, the possibility of exploring the floor of the Mawrth Vallis channel could reveal other ancient environments.

8. Summary and Conclusions

The region of Mawrth Vallis offers particularly diverse environments of deposition, alteration, and erosion, within a few tens of kilometers in multiple locations at a large site. The sequence of strata can be visited from the center of the ellipse to the floor of the Mawrth Vallis channel in the eastern part of the ellipse. Deeper rocks might be accessible in the ejecta from the 14 km diameter crater south of the site. The western part of the ellipse is less eroded and primarily exhibits the upper part of the clay-rich sequence and the dark cap, in particular on the walls of Oyama Crater. Putative ancient valleys are also present in several locations in the site. Numerous halo-bounded fractures may also indicate fluid circulation in the subsurface. Unaltered volcanic products may also be accessible in the dark cap rocks.

The Al clay-rich rocks overlie the Fe clay rocks at different levels, both at the top of the site, and down to the floor of Mawrth Vallis, pointing to an episode of alteration after the erosion by the outflow channel. Fe-rich clays are identified in all other layered rocks of the site, except in one outcrop where possible sulfates are present.

Visiting this site with a rover would provide access within a few kilometers to an extraordinary wealth and variety of geochemical processes and ancient environments. The water-related history of the region dates back to the Noachian, thus enabling the opportunity to visit for the first time the strongly altered material from this period over such a thick and large stratigraphic section. Following the degradation of the dark cap, the clay-rich unit experienced active erosion, mainly linked to wind, and hence offers relatively fresh outcrops, maximizing the chance of preserving potential biomarkers.

References

- Bibring, J.-P., *et al.* (2004), OMEGA: Observatoire pour la Minéralogie, l'Eau, les Glaces et l'Activité, in *Mars Express: The Scientific Payload, Sci. Coordination: Agustin Chicarro. ESA SP-1240*, edited by A. Wilson, pp. 37–49, ESA Publications Division, Noordwijk, Netherlands.
- Bibring, J.-P., Y. Langevin, J. F. Mustard, F. Poulet, R. Arvidson, A. Gendrin, B. Gondet, N. Mangold, P. Pinet, and F. Forget (2006), Global mineralogical and aqueous Mars history derived from OMEGA/Mars Express Data, *Science*, 312(5772), 400–404, doi:10.1126/science.1122659.
- Bishop, J. L., *et al.* (2008), Phyllosilicate diversity and past aqueous activity revealed at Mawrth Vallis, Mars, *Science*, 321, 830, doi:10.1126/science.1159699.
- Bishop, J. L., D. Loizeau, N. K. McKeown, S. Lee, M. Darby Dyar, D. J. Des, M. P. Marais, and S. L. Murchie (2013), What the ancient phyllosilicates at Mawrth Vallis can tell us about possible habitability on early Mars, *Planet. Space Sci.*, 86, 130–149, doi:10.1016/j.pss.2013.05.006.
- Carter, J., D. Loizeau, N. Mangold, F. Poulet, and J.-P. Bibring (2015), Widespread surface weathering on early Mars: A case for a warmer and wetter climate, *Icarus*, 248, 373–382, doi:10.1016/j.icarus.2014.11.011.

Acknowledgments

The research leading to these results has received funding from the European Research Council under the European Union's Seventh Framework Program (FP7/2007-2013)/ERC grant agreement 280168. Thanks are also given to NASA's MDAP program. We would like to thank Stephanie Werner, Jorge Vago, and John Carter for fruitful discussions concerning this study, as well as James Skinner and an anonymous reviewer who helped improving a lot the manuscript. All orbital data sets used in this study are available at the Mars Orbital Data Explorer of the Washington University in Saint Louis (<http://ode.rsl.wustl.edu/mars/>), except the HRSC DTM mosaic, available at this address: <http://europlanet.dlr.de/node/index.php?id=353>.

- Ehlmann, B. L., J. F. Mustard, S. L. Murchie, J.-P. Bibring, A. Meunier, A. A. Fraeman, and Y. Langevin (2011), Subsurface water and clay mineral formation during the early history of Mars, *Nature*, *479*(7371), 53–60, doi:10.1038/nature10582.
- El-Maarry, M. R., W. A. Watters, N. K. McKeown, J. Carter, E. Z. Noe Dobrea, J. L. Bishop, A. Pommerol, and N. Thomas (2014), Potential desiccation cracks on Mars: A synthesis from modeling, analogue-field studies, and global observations, paper presented at Lunar Planet. Sci. Conf. XLV, The Woodlands, Tex., Abstract 2530.
- Farrand, W. H., T. D. Glotch, J. W. Rice, J. A. Hurowitz, and G. A. Swayze (2009), Discovery of jarosite within the Mawrth Vallis region of Mars: Implications for the geologic history of the region, *Icarus*, *204*(2), 478–488, doi:10.1016/j.icarus.2009.07.014.
- Farrand, W. H., T. D. Glotch, and B. Horgan (2014), Detection of copiapite in the northern Mawrth Vallis region of Mars: Evidence of acid sulfate alteration, *Icarus*, *241*, 346–357, doi:10.1016/j.icarus.2014.07.003.
- Ferguson, R. L., P. R. Christensen, and H. H. Kieffer (2006), High-resolution thermal inertia derived from the Thermal Emission Imaging System (THEMIS): Thermal model and applications, *J. Geophys. Res.*, *111*, E12004, doi:10.1029/2006JE002735.
- Gaudin, A., E. Dehouck, and N. Mangold (2011), Evidence for weathering on early Mars from a comparison with terrestrial weathering profiles, *Icarus*, *216*(1), 257–268, doi:10.1016/j.icarus.2011.09.004.
- Golombek, M. (2011), Update on landing site characterization. Fifth MSL Landing Site Workshop Doubletree Hotel, Monrovia, Calif., 16–18 May 2011. [Available at http://marsoweb.nas.nasa.gov/landingsites/msl/workshops/5th_workshop/program.html]
- Golombek, M., et al. (2012), Selection of the Mars Science Laboratory landing site, *Space Sci. Rev.*, *170*(1–4), 641–737, doi:10.1007/s11214-012-9916-y.
- Gwinner, K., J. Oberster, R. Jaumann, and G. Neukum (2010), Regional HRSC multi-orbit digital terrain models for the Mars Science Laboratory candidate landing sites, *Proc. Lunar Planet. Sci. Conf. 41st*, held March 1–5, 2010 in The Woodlands, Tex., LPI Contribution 1533, p. 2727.
- Gwinner, K., et al. (2015), The first quadrangle of the Mars Express HRSC Multi Orbit Data Products (MC-11-E), European Planetary Science Congress EPSC2015-672.
- Hartmann, W. K., and G. Neukum (2001), Cratering chronology and the evolution of Mars, *Space Sci. Rev.*, *96*, 165–194.
- Horgan, B., J. A. Kahlmann-Robinson, J. L. Bishop, and P. R. Christensen (2013), Climate change and a sequence of habitable ancient surface environments preserved in pedogenically altered sediments at Mawrth Vallis, Mars, paper presented at Lunar Planet. Sci. Conf., The Woodlands, Tex., Abstract 3059.
- Ivanov, B. A. (2001), Mars/Moon cratering rate ratio estimates, *Space Sci. Rev.*, *96*, 87–104.
- Le Deit, L., J. Flahaut, C. Quantin, E. Hauber, D. Mège, O. Bourgeois, J. Gurgurewicz, M. Massé, and R. Jaumann (2012), Extensive surface pedogenic alteration of the Martian Noachian crust suggested by plateau phyllosilicates around Valles Marineris, *J. Geophys. Res.*, *117*, E00J05, doi:10.1029/2011JE003983.
- Loizeau, D., et al. (2007), Phyllosilicates in the Mawrth Vallis region of Mars, *J. Geophys. Res.*, *112*, E08S08, doi:10.1029/2006JE002877.
- Loizeau, D., N. Mangold, F. Poulet, V. Ansan, E. Hauber, J.-P. Bibring, B. Gondet, Y. Langevin, P. Masson, and G. Neukum (2010), Stratigraphy in the Mawrth Vallis region through OMEGA, HRSC color imagery and DTM, *Icarus*, *205*(2), 396–418, doi:10.1016/j.icarus.2009.04.018.
- Loizeau, D., S. C. Werner, N. Mangold, J.-P. Bibring, and J. L. Vago (2012), Chronology of deposition and alteration in the Mawrth Vallis region, *Mars. Planet. Space Sci.*, *72*(1), 31–43, doi:10.1016/j.pss.2012.06.023.
- Malin, M. C., et al. (2007), Context Camera investigation on board the Mars Reconnaissance Orbiter, *J. Geophys. Res.*, *112*, E05S04, doi:10.1029/2006JE002808.
- Mangold, N., et al. (2011), Targets to address MSL goals and major Martian science objectives at Mawrth Vallis Fifth MSL Landing Site Workshop, Doubletree Hotel, Monrovia, Calif., 16–18 May 2011. [Available at http://marsoweb.nas.nasa.gov/landingsites/msl/workshops/5th_workshop/program.html]
- McEwen, A. S., et al. (2007), Mars Reconnaissance Orbiter's High Resolution Imaging Science Experiment (HiRISE), *J. Geophys. Res.*, *112*, E05S02, doi:10.1029/2005JE002605.
- McKeown, N. K., J. L. Bishop, E. Z. Noe Dobrea, B. L. Ehlmann, M. Parente, J. F. Mustard, S. L. Murchie, G. A. Swayze, J.-P. Bibring, and E. A. Silver (2009), Characterization of phyllosilicates observed in the central Mawrth Vallis region, Mars, their potential formational processes, and implications for past climate, *J. Geophys. Res.*, *114*, E00D10, doi:10.1029/2008JE003301.
- McKeown, N. K., J. L. Bishop, and E. A. Silver (2013), Variability of rock texture and morphology correlated with the clay-bearing units at Mawrth Vallis, Mars, *J. Geophys. Res. Planets*, *118*, 1245–1256, doi:10.1002/jgre.20096.
- Mars Sample Return End-to-End International Science Analysis Group (2011), Planning for Mars returned sample science: Final report of the MSR End-to-End International Science Analysis Group (E2E-iSAG), *Astrobiology*, *12*, 175–230.
- Michael, G. G., and G. Neukum (2010), Planetary surface dating from crater size-frequency distribution measurements: Partial resurfacing events and statistical age uncertainty, *Earth Planet. Sci. Lett.*, *294*, 223–229.
- Michalski, J. R., and E. Z. Noe Dobrea (2007), Evidence for a sedimentary origin of clay minerals in the Mawrth Vallis region, Mars, *Geology*, *35*(10), 951–954, doi:10.1130/G23854A.1.
- Michalski, J. R., et al. (2010), The Mawrth Vallis region of Mars: A potential landing site for the Mars Science Laboratory (MSL) mission, *Astrobiology*, *10*(7), 687–703, doi:10.1089/ast.2010.0491.
- Michalski, J. R., P. B. Niles, J. Cuadros, and A. M. Baldridge (2013), Multiple working hypotheses for the formation of compositional stratigraphy on Mars: Insights from the Mawrth Vallis region, *Icarus*, *226*(1), 816–840, doi:10.1016/j.icarus.2013.05.024.
- Murchie, S., et al. (2007), Compact Reconnaissance Imaging Spectrometer for Mars (CRISM) on Mars Reconnaissance Orbiter (MRO), *J. Geophys. Res.*, *112*, E05S03, doi:10.1029/2006JE002682.
- Mustard, J. F., et al. (2013), Report of the Mars 2020 science definition team, 154 pp., posted July, 2013, by the Mars Exploration Program Analysis Group (MEPAG). [Available at http://mepag.jpl.nasa.gov/reports/MEP/Mars_2020_SDT_Report_Final.pdf]
- Neukum, G., et al. (2004), HRSC: The High Resolution Stereo Camera of Mars Express, in *Mars Express: The Scientific Payload, Sci. Coord.: Agustin Chicarro. ESA SP-1240*, edited by A. Wilson, pp. 17–35, ESA Publications Division, Noordwijk, Netherlands.
- Noe Dobrea, E. Z., et al. (2010), Mineralogy and stratigraphy of phyllosilicate-bearing and dark mantling units in the greater Mawrth Vallis/west Arabia Terra area: Constraints on geological origin, *J. Geophys. Res.*, *115*, E00D19, doi:10.1029/2009JE003351.
- Noe Dobrea, E. Z., J. R. Michalski, and G. Swayze (2011), Aqueous mineralogy and stratigraphy at and around the proposed Mawrth Vallis MSL Landing Site: New insights into the aqueous history of the region, *Mars*, *6*, 32–46, doi:10.1555/mars.2011.0003.
- Okubo, C. H., and A. S. McEwen (2007), Fracture-Controlled Paleo-Fluid Flow in Candor Chasma, Mars, *Science*, *315*(5814), 983–985, doi:10.1126/science.1136855.
- Poulet, F., J.-P. Bibring, J. F. Mustard, A. Gendrin, N. Mangold, Y. Langevin, R. E. Arvidson, B. Gondet, and C. Gomez (2005), Phyllosilicates on Mars and implications for early Martian climate, *Nature*, *438*(7068), 623–627, doi:10.1038/nature04274.
- Poulet, F., N. Mangold, D. Loizeau, J.-P. Bibring, Y. Langevin, J. R. Michalski, and B. Gondet (2008), Abundance of minerals in the phyllosilicate-rich units on Mars, *Astron. Astrophys.*, *487*, L41–L44, doi:10.1051/0004-6361/200810150.

- Poulet, F., J. Carter, J. L. Bishop, D. Loizeau, and S. M. Murchie (2014), Mineral abundances at the final four Curiosity study sites and implications for their formation, *Icarus*, *231*, 65–76, doi:10.1016/j.icarus.2013.11.023.
- Tanaka, K. L., J. A. Skinner, J. M. Dohm, R. P. Irwin, E. J. Kolb, C. M. Fortezzo, T. Platz, G. G. Michael, and T. M. Hare (2014), Geologic map of Mars, Scientific Investigations Map 3292. U.S. Geol. Sur., doi:10.3133/sim3292.
- Wray, J. J., B. L. Ehlmann, S. W. Squyres, J. F. Mustard, and R. L. Kirk (2008), Compositional stratigraphy of clay-bearing layered deposits at Mawrth Vallis, Mars, *Geophys. Res. Lett.*, *35*, L12202, doi:10.1029/2008GL034385.
- Wray, J. J., S. W. Squyres, L. H. Roach, J. L. Bishop, J. F. Mustard, N. Dobrea, and Z. Eldar (2010), Identification of the Ca-sulfate bassanite in Mawrth Vallis, Mars, *Icarus*, *209*(2), 416–421, doi:10.1016/j.icarus.2010.06.001.